Journal of Engineering Mathematics (2006) 54: 225–259
DOI 10.1007/s10665-005-7720-3

Operating charts for continuous sedimentation III: control of step inputs

STEFAN DIEHL
Centre for Mathematical Sciences, Lund University, P.O. Box 118, SE-221 00 Lund, Sweden (e-mail: diehl@maths.lth.se)

Received 28 June 2004; accepted in revised form 10 May 2005 / Published online: 19 May 2006

Abstract. The main purposes of a clarifier-thickener unit is that it should produce a high underflow concentration and a zero effluent concentration. The main difficulty in the control of the clarification-thickening process (by adjusting a volume flow) is that it is nonlinear with complex relations between concentrations and volume flows via the solution of a PDE – a conservation law with a source term and a space-discontinuous flux function. In order to approach this problem, control objectives for dynamic operation and strategies on how to meet these objectives are presented in the case when the clarifier-thickener unit initially is in steady state in optimal operation and is subjected to step input data. A complete classification of such solutions is given by means of an operating chart (concentration-flux diagram).

Key words: continuous sedimentation, control, operating charts, step response, thickener

1. Introduction

The process of continuous sedimentation of particles in a liquid has received considerable attention during the last century. There are many publications ranging from experiments to rigorous mathematical modelling. For many purposes simplified one-dimensional models are mostly considered and desired for simulation, control and design of plants. We refer to the preceding papers in this series [1, 2] for references and discussions of previous works. For the particular problem of controlling the process, different angles of approach can be found in [3–9].

The one-dimensional model for an ideal clarifier-thickener can be written as a partial differential equation that conserves mass (conservation law). Different types of modelling problems arise. One is the settling and compressible behaviour of the particles, reflected in the constitutive relation between the settling flux (mass per unit of time and unit area) and the concentration and other physical variables. Other problems are the mathematical difficulties that arise due to the discontinuities of the flux function at the inlet and outlets of the sedimentation vessel. In [1, 2] it was motivated why it is important to continue to examine all consequences of the fundamental constitutive assumption by Kynch, although it does not take into account the compressible behaviour for high concentrations shown by many suspensions. A further motivation for the present paper is that a systematic analysis of the control possibilities and limitations of the process cannot be found in the literature.

The aim of the present series of articles is to provide deeper knowledge of the continuous-sedimentation process for all possible input data and to show how the process can be controlled. This is done by classifying the nonlinear behaviour by means of operating charts. In [1] all qualitatively different steady-state solutions and several relations between the different variables were presented. Control objectives were also suggested. Since the process is hardly

ever in complete steady state, it is not sufficient to have control objectives formulated only in terms of steady-state solutions. In [2] the state of optimal operation was defined as a class of dynamic solutions. Furthermore, all qualitatively different step responses were classified for the case when the settler is in optimal operation initially and the control variable (the volume underflow rate) is held constant. The same initial conditions are assumed in the present paper and all theoretically possible step inputs are considered. In addition, the control variable is now adjusted.

The paper is organized as follows. Sections 2 and 3 contain the necessary previous results and notation. Control objectives for dynamic solutions are formulated in Section 4 and strategies on how to satisfy these are introduced in Section 5. A control strategy is called optimal if the given control objective is satisfied. To establish optimal control strategies, the first step is to investigate dynamic solutions when there is a direct control action (a step change in the control variable). These solutions are presented and classified in Section 6. Although the value of the control variable in each case corresponds to a desired steady-state solution, the control objectives are not satisfied in all cases. Hence, more advanced control strategies are needed to meet the control objectives. The main results of the paper are the optimal control strategies presented in Section 7.

2. The clarifier-thickener unit and the model

The one-dimensional model of the clarifier-thickener unit, or settler, was first presented in [10]. The model and the full notation for constructing solutions are given in [2, Section 2], to which we now refer the reader. Here, we review only briefly the basic concepts. Although we refer to analytical solutions of the model partial differential equation, the paper can be read without going into such details and by studying the operating charts and numerical solutions instead.

Figure 1 shows the settler together with the flux function in the thickening zone. The typical and desired steady-state solution has zero concentration in the clarification zone and a

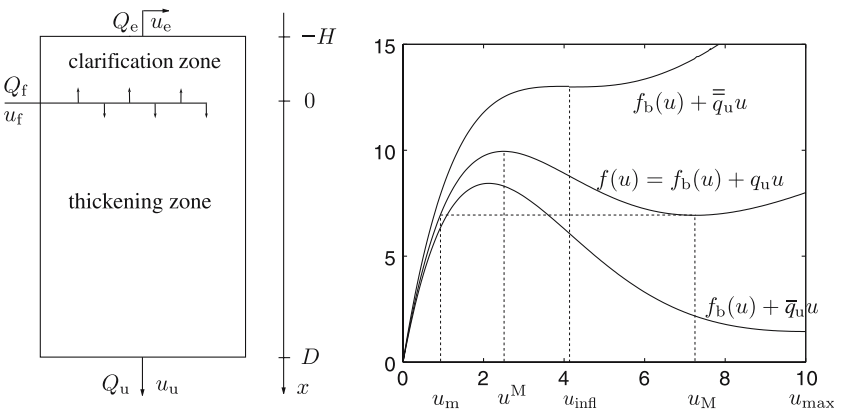

Figure 1. Left: Schematic picture of an ideal one-dimensional clarifier-thickener unit, where u stands for concentration and Q for volume flow of the feed, effluent and underflow streams, respectively. The flow restrictions are $Q_f = Q_e + Q_u > 0$ and $Q_e \geq 0$. *Right*: flux curves $f(u)$ in the thickening zone and characteristic concentrations. The bulk velocities are defined as $q_u = Q_u/A$ etc., where A is the cross-sectional area. For $\bar{q}_u < q_u < \bar{\bar{q}}_u$ there is a local minimum point u_M of $f(u)$ that lies between u_{infl} and u_{max}. Given u_M, u_m is the lower concentration defined by $f(u_m) = f(u_M)$, u^M is the (local) maximum point of $f(u)$, u_{infl} is the inflection point of $f_b(u)$ and $f(u)$ (independent of q_u). The batch-settling flux used for the numerical simulations is $f_b(u) = 10u\big((1 - 0{\cdot}64u/u_{max})^{6{\cdot}55} - 0{\cdot}36^{6{\cdot}55}\big)$ $\big[\mathrm{kg}/(\mathrm{m}^2\mathrm{h})\big]$.

discontinuity in the thickening zone between the concentrations u_m and u_M. This is called the sludge blanket level (SBL) in wastewater treatment and it is important to be able to control it. The conservation law can be written as the partial differential equation

$$u_t + \big(F(u,x)\big)_x = s(t)\delta(x), \tag{1}$$

where δ is the Dirac measure, the total flux function is

$$F(u,x) = \begin{cases} -q_\mathrm{e}u, & x < -H \\ g(u) = f_\mathrm{b}(u) - q_\mathrm{e}u, & -H < x < 0 \\ f(u) = f_\mathrm{b}(u) + q_\mathrm{u}u, & 0 < x < D \\ q_\mathrm{u}u, & x > D \end{cases}$$

and the source function is

$$s(t) = \frac{Q_\mathrm{f}}{A}u_\mathrm{f}(t) = \frac{Q_\mathrm{u}+Q_\mathrm{e}}{A}u_\mathrm{f}(t) = (q_\mathrm{u}+q_\mathrm{e})u_\mathrm{f}(t).$$

The physical input variables are the feed concentration u_f and the feed volume flow Q_f. For graphical interpretations by means of operating charts it is, however, convenient to use the *feed point* (u_f, s) as input variable. The *control variable* of the process is Q_u. Two particular values of this variable arise from the properties of the batch-settling flux function. Define

$$\bar{q}_\mathrm{u} = -f_\mathrm{b}'(u_\mathrm{max}), \quad \bar{Q}_\mathrm{u} = \bar{q}_\mathrm{u}A,$$
$$\bar{\bar{q}}_\mathrm{u} = -f_\mathrm{b}'(u_\mathrm{infl}), \quad \bar{\bar{Q}}_\mathrm{u} = \bar{\bar{q}}_\mathrm{u}A,$$

which are the bulk velocities such that the slope of f is zero at u_max and u_infl, respectively; see Figure 1 (right).

The purposes of the settler may vary depending on the industrial process it is used for. At least in wastewater treatment the main *purposes* of the settler are the following. It should

1. produce a low effluent concentration;
2. produce a high underflow concentration;
3. work as a buffer of mass and be insensitive to small variations in the feed variables.

These purposes cannot be controlled independently.

3. Control of steady states and optimal operation

Figure 2 shows the operating chart for the steady states. Depending on the location of the feed point (u_f, s) in the steady-state chart, there are different possible steady-state solutions, which are all piecewise constant and non-decreasing with depth; see [1] for a complete table and a full notation. The *limiting flux* and the *excess flux* are defined as:

$$f_\mathrm{lim}(u) = \min_{u \le \alpha \le u_\mathrm{max}} f(\alpha) = \begin{cases} f(u), & u \in [0, u_\mathrm{m}] \cup [u_\mathrm{M}, u_\mathrm{max}], \\ f(u_\mathrm{M}), & u \in (u_\mathrm{m}, u_\mathrm{M}), \end{cases}$$
$$\mathcal{E}(u_\mathrm{f}, s) = s - f_\mathrm{lim}(u_\mathrm{f}).$$

These fluxes, as well as the characteristic concentrations and the regions of the steady-state chart depend on the control variable Q_u; *e.g.* $u_\mathrm{M}(Q_\mathrm{u})$, $f(u, Q_\mathrm{u})$, $f_\mathrm{lim}(u_\mathrm{f}, Q_\mathrm{u})$ and $\mathcal{E}(u_\mathrm{f}, s, Q_\mathrm{u})$. The following regions in the operating chart are independent on Q_u:

$$\Lambda_i = \bigcup_{Q_\mathrm{u} > 0} \ell_i(Q_\mathrm{u}), \quad i = 1, \ldots, 4,$$

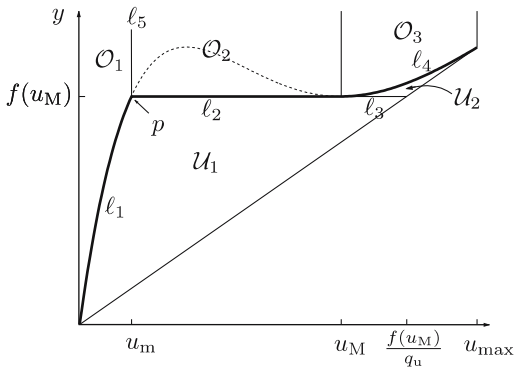

Figure 2. The steady-state chart. The thick graph is the limiting flux curve. If the feed point lies on this curve, the settler is critically loaded in steady state, which means that it works at its maximum capacity. Below this graph the settler is underloaded, and above it is overloaded with a non-zero effluent concentration. Each region corresponds to a specific steady state which is unique, except on the limiting flux curve (and on ℓ_3 and ℓ_5), where the location of a discontinuity in the thickening and/or the clarification zone is not uniquely determined. Note that the regions in this chart all depend on $Q_{\rm u}$. (They are defined in [1].)

$$P = P_1 \cup P_2, \quad \text{where} \quad P_1 = \bigcup_{0<Q_{\rm u}\le \bar{\bar{Q}}_{\rm u}} p(Q_{\rm u}), \quad P_2 = \bigcup_{Q_{\rm u}> \bar{\bar{Q}}_{\rm u}} p(Q_{\rm u});$$

see Figure 3 (right). In [1] some control objectives are formulated in order to meet the purposes stated in Section 2. It turns out that it is important to be able to have a critically loaded settler in steady state, *i.e.*, to find a value of $Q_{\rm u}$ such that $\mathcal{E}(u_{\rm f}, s, Q_{\rm u}) = 0$. The following theorem in [1] captures the most important properties in this context.

Theorem 3.1. *Given* $(u_{\rm f}, s) \in \{(u, y) : 0 < u \le u_{\max},\ y > 0\}$*, there exists a unique* $\tilde{Q}_{\rm u}(u_{\rm f}, s) > 0$ *such that* $\mathcal{E}(u_{\rm f}, s, \tilde{Q}_{\rm u}) = 0$ *and the following properties hold:*

$$(u_{\rm f}, s) \in \Lambda_i \implies (u_{\rm f}, s) \in \ell_i(\tilde{Q}_{\rm u}), \quad i = 1, 2, 4,$$
$$(u_{\rm f}, s) \in P \implies (u_{\rm f}, s) \in p(\tilde{Q}_{\rm u}),$$

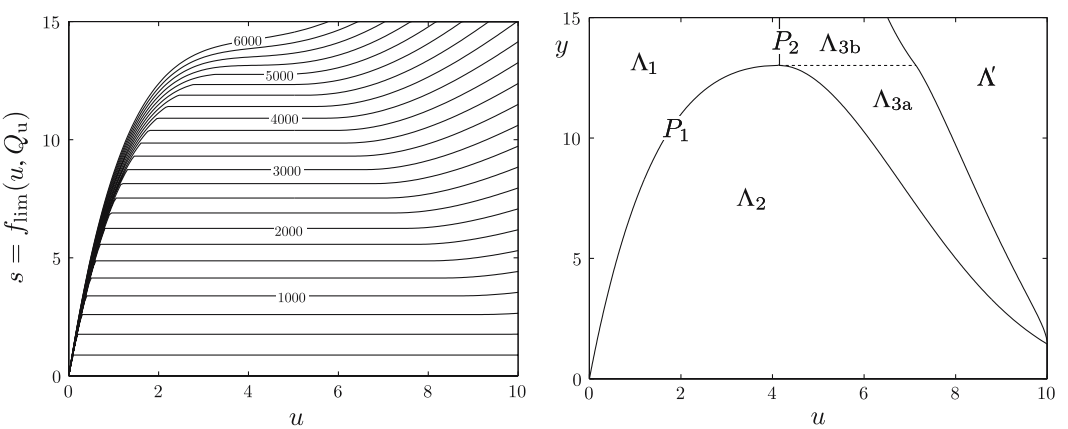

Figure 3. Operating charts for control of steady states. *Left*: Graphs of $f_{\rm lim}(\cdot, Q_{\rm u})$ for some values of $Q_{\rm u}$. *Right*: The control chart with respect to steady states; $\Lambda_3 = \Lambda_{3a} \cup \Lambda_{3b}$, $\Lambda_4 = \Lambda_3 \cup \Lambda'$. Theorem 3.1 says that, given a feed point in this chart, there is a unique graph $f_{\rm lim}(\cdot, \tilde{Q}_{\rm u})$ that passes through the feed point. With the value $\tilde{Q}_{\rm u}$ the settler is critically loaded in steady state.

$\tilde{Q}_u$ *is a continuous function on* Ω,

$\mathcal{E}(u_f, s, Q_u) \leq 0 \iff Q_u \geq \tilde{Q}_u(u_f, s)$.

If $(u_f, s) \in \Lambda_3$, *there exists a unique* $Q_u > 0$ *with* $(u_f, s) \in \ell_3(Q_u)$.

Choosing the particular value $Q_u = \tilde{Q}_u \Leftrightarrow \mathcal{E}(u_f, s, \tilde{Q}_u) = 0$ will thus yield a critically loaded settler. It can be shown that the maximum value of the underflow concentration is

$$\tilde{u}_u(u_f, s) = \frac{As}{\tilde{Q}_u(u_f, s)}, \tag{2}$$

which is a decreasing function of s for all $s > \bar{q}_u u_{max}$ and $u_f < u_{max}$. For $s \leq \bar{q}_u u_{max}$, $\tilde{u}_u(u_f, s) = u_{max}$ holds.

Consider the last statement of Theorem 3.1. For $Q_u \geq \bar{\bar{Q}}_u$, we have $u_m = u_M = u_{infl}$ and the sludge blanket deteriorates. Therefore, we divide Λ_3 into

$$\Lambda_{3a} = \Lambda_3 \cap \left\{(u, y) : y < f_b(u_{infl}) + \bar{\bar{q}}_u u_{infl}\right\} \quad \text{and} \quad \Lambda_{3b} = \Lambda_3 \setminus \Lambda_{3a}; \tag{3}$$

see Figure 3 (right).

The concept of *optimal operation in steady state* means that the concentration is zero in the clarification zone and there is a (stationary) discontinuity within the thickening zone at the depth $x = x_{sb} \in (0, D)$ – the sludge blanket level (SBL). Optimal operation in steady state is one of the main control objectives discussed in [1] and it satisfies the third purpose of the settler above.

A necessary condition for optimal operation in steady state is that $(u_f, s) \in p(Q_u) \cup \ell_2(Q_u) \cup \ell_3(Q_u)$ and $Q_u < \bar{\bar{Q}}_u$, which implies $(u_f, s) \in P_1 \cup \Lambda_2 \cup \Lambda_{3a}$; see Figure 3. Sufficient conditions for obtaining this state asymptotically involve the values of the input variables and the control variable, as well as the present concentration distribution. To obtain such conditions the dynamic behaviour needs to be charted. Since the continuous-sedimentation process is hardly ever in complete steady state, it is not sufficient to have control objectives only formulated in terms of steady-state solutions. Therefore, we also need a general definition of optimal operation. Let u_{cl} denote the restriction of the solution u to the clarification zone.

Definition 3.1. *The settler is said to be in* optimal operation *at time* t *if* $Q_u(t) < \bar{\bar{Q}}_u$ *and the solution of* (1) *satisfies:*

- $u_{cl}(x, t) = 0 \Leftrightarrow u(x, t) = 0, \quad -H < x < 0,$
- *there exists a level* $x_{sb}(t) \in (0, D)$ *such that*

$$u(x, t) \in \begin{cases} [0, u_{infl}), & 0 < x < x_{sb}(t) \\ [u_{infl}, u_{max}], & x_{sb}(t) < x < D. \end{cases}$$

Hence, we have a natural definition of the SBL for a settler in optimal operation: it is the discontinuity at the level $x = x_{sb}(t)$ in the thickening zone, such that the jump in the concentration passes the characteristic concentration u_{infl}.

4. Control objectives

The three purposes of the settler in Section 2 can be written in terms of the solution of (1), namely the two output concentrations and the concentration distribution in the settler:

Table 1. Control objectives. For each control objective the first condition should be maintained as long as possible. After that, the next condition should be met as long as possible, etc.

Objective	1st condition	2nd condition	3rd condition
CO1	Optimal operation	$u_{cl}=0$	
CO2	Optimal operation	$u_u \geq u_u^{min}$ subject to $u_e=0$	$u_e=0$
CO3	Optimal operation subject to $u_u \geq u_u^{min}$	$u_u \geq u_u^{min}$ subject to $u_e=0$	$u_e=0$
CO4	u_u is maximized subject to $u_e=0$		

1. $u_e(t)=0$;
2. $u_u(t)$ is maximized or bounded below;
3. the settler is in optimal operation.

With our definition of optimal operation, purpose 1 is a subset of purpose 3. As regards steady-state situations, we know from [1] that purpose 2 is fulfilled as Q_u is minimized. Purpose 1, on the other hand, is satisfied as Q_u is sufficiently high. The boundary case, in which purposes 1 and 2 are fulfilled, is when the settler is critically loaded in steady state, which can always be attained according to Theorem 3.1. Optimal operation is also an intermediate state; however, it is not equivalent to a critically loaded settler. The extra advantages of purpose 3 are the buffer and robustness properties of the settler.

As we shall see, for high loads optimal operation cannot be maintained infinitely long. Therefore, given a lower bound u_u^{min} on the underflow concentration, we define the *control objectives* in Table 1. When optimal operation cannot be maintained, a second condition comes into effect, and if this can only be satisfied during a finite time, a third condition takes effect. Thereby, all four objectives can always be met (with the natural interpretation $Q_u=Q_f \Leftrightarrow Q_e=0$ means that $u_e=0$). In CO4, particles are allowed in the clarification zone at any time, but in CO2 and CO3 only upon failure of optimal operation. This limits the mass-buffer property of the settler and increases the risk of an overflow due to disturbances. Thus, there are major disadvantages with CO4 in comparison to the other objectives. CO4 can only be 'advantageous' during transient periods in the sense that $u_u(t)$ may be slightly higher than its maximum value in steady state, $\tilde{u}_u$ (see Equation (2)). Therefore, we do not consider CO4 in this paper. Note that CO3 is the same as CO2 plus the constraint that $u_u(t)$ is always bounded from below. This can be described *a priori* in terms of the control variable during favourable conditions; see Theorem 4.1 and Figure 4.

Theorem 4.1. *Assume that the settler is in optimal operation for* $0 \leq t \leq T$.

- *The underflow concentration satisfies* $u_u(t) \in \left(\bar{\bar{u}}_u, u_{max}\right]$ *for* $0 \leq t \leq T$, *where* $\bar{\bar{u}}_u = f(u_{infl}, \bar{\bar{Q}}_u)/\bar{\bar{q}}_u$.
- *Let* $u_u^{min} \in (\bar{\bar{u}}_u, u_{max})$ *be a given desired lower bound on the underflow concentration. Assume that* $Q_u(t) \leq Q_u^{max1}$, *where* Q_u^{max1} *is defined*[1] *uniquely by*

$$f\left(u_M(Q_u^{max1}), Q_u^{max1}\right) = \frac{Q_u^{max1}}{A} u_u^{min}.$$

Then $u_u(t) \geq u_u^{min}$ *for* $0 \leq t \leq T$ *and* $Q_u^{max1} > \bar{Q}_u$.

[1]The notation Q_u^{max} will be used, in the subsequent paper in this series, for a more general upper bound of the control variable in connection with a regulator.

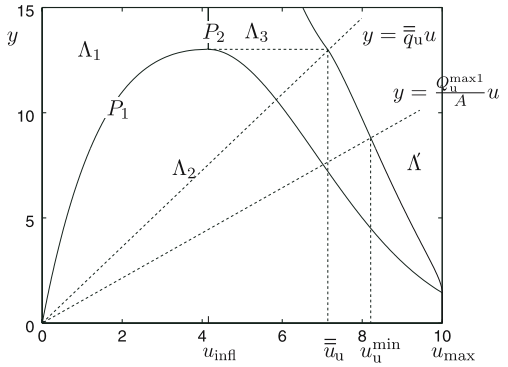

Figure 4. The characteristic concentrations of Theorem 4.1 can be obtained graphically in the operating chart for control of steady states. $\bar{\bar{u}}_u \approx 7{\cdot}13$ kg/m^3 satisfies $f(u_{infl}, \bar{\bar{Q}}_u) = \bar{\bar{q}}_u \bar{\bar{u}}_u$. $Q_u^{max\,1}$ can be obtained graphically in the following way. Given $u_u^{min} \in (\bar{\bar{u}}_u, u_{max}]$ determine the corresponding y-value on the boundary of Λ_3 and Λ'. This flux value is equal to $Q_u^{max\,1} u_u^{min}/A$.

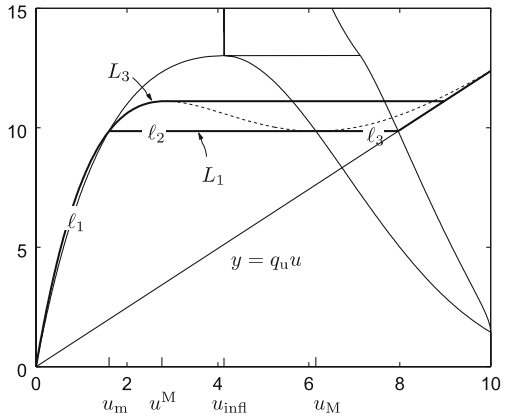

Figure 5. The sets L_1 and L_3. Note that the feed point lies on the line $y = q_u u$ if and only if $Q_e = 0 \Leftrightarrow Q_u = Q_f$.

Proof. The definition of optimal operation means that $Q_u \in (0, \bar{\bar{Q}}_u)$ and that, for every fixed $t \in [0, T]$, the limit bottom concentration satisfies $u_D \equiv u(D-0, t) \in [u_{infl}, u_{max}]$. The boundary limit given by [2, Equation (6)] implies $u^D(t) \equiv \lim_{\varepsilon \searrow 0} u_D(t+\varepsilon) \in \big[u_M(Q_u), u_{max}\big]$. The underflow concentration is then given by [2, Equation (8)]:

$$u_u(t) = \frac{f\big(u^D(t)\big)}{q_u} = u^D(t) + \frac{A f_b\big(u^D(t)\big)}{Q_u}, \tag{4}$$

which defines a continuously differentiable function $u_u(u^D, Q_u)$ for fixed t. We have

$$\frac{\partial u_u}{\partial u^D} = 1 + \frac{A f_b'(u^D)}{Q_u} = \frac{Q_u}{A} f'(u^D) \geq 0, \quad u^D \in \big[u_M(Q_u), u_{max}\big].$$

Hence, for each $Q_u \in (0, \bar{\bar{Q}}_u)$,

$$\min_{u^D \in [u_M(Q_u), u_{max}]} u_u(u^D, Q_u) = u_u\big(u_M(Q_u), Q_u\big) \overset{(4)}{=} u_M(Q_u) + \frac{A f_b\big(u_M(Q_u)\big)}{Q_u}.$$

We investigate the latter relation between u_u and Q_u. For $0 < Q_u \leq \bar{Q}_u$ we have

$$u_u\big(u_M(Q_u), Q_u\big) = u_u(u_{max}, Q_u) = u_{max} + \frac{A f_b(u_{max})}{Q_u} = u_{max}.$$

For $\bar{Q}_u < Q_u < \bar{\bar{Q}}_u$ we can use the fact that $\dfrac{d}{dQ_u} f\big(u_M(Q_u), Q_u\big) = u_M(Q_u)/A < u_{max}/A$, see (A2) in [1], to conclude that

$$\frac{d}{dQ_u} u_u\big(u_M(Q_u), Q_u\big) = -\frac{A}{Q_u^2} f\big(u_M(Q_u), Q_u\big) + \frac{A}{Q_u} \frac{d}{dQ_u} f\big(u_M(Q_u), Q_u\big) =$$
$$= \frac{A}{Q_u^2} \left(-f\big(u_M(Q_u), Q_u\big) + \frac{Q_u}{A} u_M(Q_u) \right) = -\frac{A f_b\big(u_M(Q_u)\big)}{Q_u^2} < 0.$$

Thus, the continuous function $u_u\big(u_M(Q_u), Q_u\big)$ of Q_u is decreasing for $\bar{Q}_u \le Q_u < \bar{\bar{Q}}_u$ taking all values from u_{max} down to

$$u_u\big(u_M(\bar{\bar{Q}}_u), \bar{\bar{Q}}_u\big) = u_u\big(u_{infl}, \bar{\bar{Q}}_u\big) = u_{infl} + \frac{A f_b(u_{infl})}{\bar{\bar{Q}}_u} = \frac{f(u_{infl}, \bar{\bar{Q}}_u)}{\bar{\bar{q}}_u} = \bar{\bar{u}}_u.$$

Hence, for given $u_u^{min} \in (\bar{\bar{u}}_u, u_{max})$ there exists a unique value $Q_u^{max1} > \bar{Q}_u$ such

$$u_u^{min} = u_u\big(u_M(Q_u^{max1}), Q_u^{max1}\big) = u_M(Q_u^{max1}) + \frac{A f_b\big(u_M(Q_u^{max1})\big)}{Q_u^{max1}},$$

which after multiplying by Q_u^{max1}/A finishes the proof.

5. Control strategies

Assume that the feed point $\big(u_f(t), s(t)\big)$ moves around, continuously and/or discontinuously, in the operating chart. To fulfil any control objective, control strategies need to be specified, which means that Q_u is defined as a function of the feed point and time. By a control action we mean a relation between Q_u and (u_f, s) at a fixed time point. In order to propose control strategies we define the following subsets, or *lines*, in the operating chart:

$$L_1 = \bigcup_{i=1}^{3} \ell_i \cup p \cup \left\{(u, y) : y = q_u u, \frac{f(u_M)}{q_u} < u \le u_{max}\right\},$$

$$L_2 = \big\{(u, y) : y = f_{lim}(u)\big\} = \ell_1 \cup p \cup \ell_2 \cup \ell_4,$$

$$L_3 = \big\{(u, y) : y = f_3(u)\big\} \quad \text{where} \quad f_3(u) = \begin{cases} f(u), & 0 \le u \le u^M \\ f(u^M), & u^M < u \le \frac{f(u^M)}{q_u} \\ q_u u, & \frac{f(u^M)}{q_u} < u \le u_{max}. \end{cases}$$

Note that these sets depend on Q_u, for example, $(u_f, s) \in L_2(Q_u)$ means that the settler is critically loaded in the corresponding steady state. L_1 and L_3 are shown in Figure 5. Some *control strategies* are the following:

DCL1: direct control with respect to L_1, *i.e.*, define $Q_u(t)$ such that $\big(u_f(t), s(t)\big) \in L_1\big(Q_u(t)\big)$; DCL2 and DCL3 are defined analogously;

PCC: piecewise constant control of $Q_u(t)$ where decisions are made depending both on the location of the feed point in the operating chart and the actual concentration distribution in the settler, especially the SBL.

Thus, for the step inputs in this paper, DC means that a single step control action is performed at $t = 0$. Omitting the initials DC means that the control action is performed at a later time point. Strategy DCL2 is motivated by the results on the control of steady states in [1] and can always be accomplished according to Theorem 3.1. With a small adjustment of the proof of that theorem, it is easy to establish that strategies DCL1 and DCL3 can always be accomplished with a unique value of Q_u for each given feed point. It is convenient to use the notation $Q_u = L_1^{-1}(u_f, s) \Leftrightarrow (u_f, s) \in L_1(Q_u)$, etc. Strategy DCL1 is equal to DCL2 for feed points in $P \cup \Lambda_2$. For $(u_f, s) \in \Lambda_3 \subset \Lambda_4$ there is a choice between making a control action with respect to a critically loaded settler, $Q_u = \ell_4^{-1}(u_f, s)$, which is DCL2, and setting the slightly higher value $Q_u = \ell_3^{-1}(u_f, s)$, which is DCL1 and aims at keeping the state optimal operation as long as possible. If $(u_f, s) \in \Lambda'$, there are similarly two alternatives. As we shall see later,

optimal operation can, however, only be maintained during a finite time in the corresponding steady state.

In Section 6 we show that DCL1 is better than DCL2 with respect to CO1 for the control of step responses. An advantage of DCL1 and DCL2 over PCC is that these ignore the present concentration distribution in the settler. A drawback of DCL2 (and similarly for DCL1) is that $Q_u(t)$ is only implicitly defined by the nonlinear equation $\mathcal{E}(u_f, s, Q_u) = 0$, which generally has to be solved numerically for $Q_u = \tilde{Q}_u$. In practice it may also take some time to realize a new flow value. Therefore, these strategies cannot be realized exactly. The simplicity of the strategy PCC – adjust the control parameter only at certain time points and keep it constant in between – is obvious and in many waste-water treatment plants the only possibility in practice. In Section 7 the strategy PCC will be specified further concerning the control of step responses. As we shall see, this strategy is sufficient for fulfilling CO1 or CO2 and the strategies DCL2 and DCL1 may actually be disadvantageous. The use of strategy DCL3 is also demonstrated in Section 7.

6. Direct control of step inputs

6.1. Operating chart for direct control of step inputs

Assume that the settler is in optimal operation and steady state initially, that there is a step change at $t = 0$ in the feed variables, and that these are constant thereafter. In this section we present the solution to a single-step control action which is performed directly. Since we aim at a stationary settler in optimal operation, only the control actions DCL1 and DCL2 will be considered in this section. The advantage of DCL1 over DCL2 will be emphasized in Sections 6.3, 6.5 and 6.7. It turns out that the qualitatively different cases depend on the underloaded region, denoted by $\mathcal{U} = \mathcal{U}_1 \cup \ell_3 \cup \mathcal{U}_2$, the overloaded region, $\mathcal{O} = \mathcal{O}_1 \cup \ell_5 \cup \mathcal{O}_2 \cup \mathcal{O}_3$, and on the control chart in Figure 3 (right). In the latter the set Λ' now has to be divided further depending on whether $s \lessgtr f(u^M)$ *after* the control action DCL1. Since the value of the control variable can be written in terms of the feed variables, $Q_u = Q_f = As/u_f$, the set Λ' can be divided beforehand:

$$\Lambda'_a = \left\{(u, y) \in \Lambda' : y \le f\left(u^M(Ay/u);\, Ay/u\right)\right\},$$
$$\Lambda'_b = \Lambda' \setminus \Lambda'_a;$$

see Figure 6, where these sets are shown (above the line $y = q_u u$). This means that the intersection of the line $y = q_u u$ and the dividing curve between Λ'_a and Λ'_b occurs at the height of the local maximum of f, *i.e.*, $f(u^M)$.

As for the construction of solutions, we omit many details as well as some auxiliary figures of flux functions. The principles have been demonstrated in the previous paper [2]. The index $_0$ denotes the value of a variable at $t = 0-$. Recall that the time-dependent variables are defined to be continuous from the right, for example, $u_{f0} = u_f(0-) \neq u_f(0+) = u_f(0)$. Variables written without the zero index correspond to constant values in the new steady state, which may arise after a finite or infinite time. Since the control parameter makes a jump at $t = 0$ from Q_{u0} to Q_u, we need to differentiate between the initial flux $f_0(\cdot) \equiv f(\cdot; Q_{u0})$ and the new one $f(\cdot) \equiv f(\cdot; Q_u)$. For variables that vary continuously during the transient period, or some part of it, the time dependence is written out, for example, $m(t)$ or $u_e(t)$. Their values in the new steady state are then written out explicitly, for example, $m(t_5)$ is the constant mass for $t \ge t_5$, and we write $u_{e\infty}$ for an asymptotic value.

6.1.1. *Initial conditions*

The settler is initially in optimal operation at steady state, *i.e.*, the feed point $(u_{f0}, s_0) \in p \cup \ell_2 \cup \ell_3$, there is zero concentration in the clarification zone and a sludge blanket in the thickening zone at the depth x_{sb0} with the concentration u_{m0} above and u_{M0} below it. The total mass in the settler is thus initially

$$m_0 = A\big(x_{sb0}u_{m0} + (D - x_{sb0})u_{M0}\big). \tag{5}$$

6.1.2. *Numerical data and simulations*

The following numerical data are used throughout the paper:

$H = 1\,\mathrm{m}$, $u_{max} = 10\,\mathrm{kg/m^3}$,
$D = 4\,\mathrm{m}$, $u_{infl} = 4{\cdot}15\,\mathrm{kg/m^3}$,
$A = \pi(30\,\mathrm{m})^2 = 2827\,\mathrm{m^2}$, $x_{sb0} = 2\,\mathrm{m}$ (unless otherwise stated).

Note that the initial mass depends on the values of u_{m0} and u_{M0}, which depend on $Q_{u0} = Q_u$. The latter variable is, for clarity, set to different values in the different cases below, which means that the initial mass is different, too. We only show the interesting cases when $Q_u < \bar{\bar{Q}}_u = 5161\ \mathrm{m^3/h}$; *cf.* Figure 3 (left). The batch-settling flux $f_b(u)$ used is shown in Figure 1 (right). The three-dimensional graphs are obtained by the numerical method described in [11]. Unless otherwise stated, the initial data are

$Q_{u0} = 3500\,\mathrm{m^3/h}$, $s_0 = 9{\cdot}86\,\mathrm{kg/(m^2h)}$,
$u_{m0} = 1{\cdot}61\,\mathrm{kg/m^3}$, $u_{M0} = 6{\cdot}16\,\mathrm{kg/m^3}$,
$u_{u0} = 7{\cdot}96\,\mathrm{kg/m^3}$, $u_{m0} < u_{f0} \le u_{M0}$;

cf. Figure 7. In the cases below we thus assume that $s_0 > \bar{q}_u u_{max} = 1{\cdot}45\,\mathrm{kg/(m^2h)}$. Otherwise, $u_{M0} = u_{u0} = u_{max}$ and some of the inequalities become equalities. In all cases in this section the effluent concentration is zero. We do not show simulation graphs of this or the evolution of the mass.

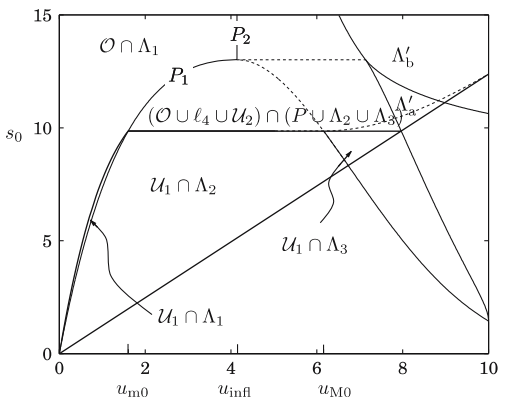

Figure 6. The operating chart for direct control of step inputs shows the regions (within the solid lines) of the qualitatively different solutions. The sets refer to the initial value Q_{u0}, *i.e.*, $\mathcal{O} \equiv \mathcal{O}(Q_{u0})$ etc. Recall that $P_1 \cup P_2 = P$.

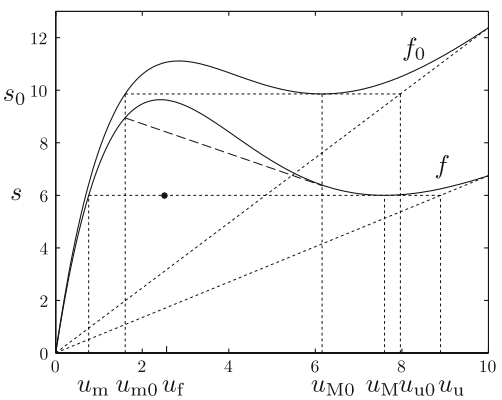

Figure 7. $(u_f, s) = (2{\cdot}5, 6{\cdot}0) \in \mathcal{U}_1(Q_{u0}) \cap \Lambda_2$. The graphs of the initial flux $f_0(\cdot) \equiv f(\cdot; Q_{u0})$ and the new one $f(\cdot) \equiv f(\cdot; Q_u)$.

6.2. $(u_f, s) \in \mathcal{U}_1(Q_{u0}) \cap (P \cup \Lambda_2)$

Suppose the new feed point is $(u_f, s) = (2{\cdot}5, 6{\cdot}0) \in \mathcal{U}_1(Q_{u0}) \cap \Lambda_2$; see Figure 7. According to DCL1 = DCL2 we let $Q_u = \tilde{Q}_u \approx 1908$, which implies $(u_f, s) \in \ell_2(Q_u)$. As we shall see, the settler will be kept in optimal operation. The graphs of the initial and the new flux functions for the thickening zone are shown in Figure 7 together with some concentrations that appear in the solution. According to Condition Γ the boundary values are $u^-(t) = 0$, $u^+(t) = u_m$ and $u^D(t) = u_M$ for $t \geq 0$. The solution is shown in Figure 8. (The slopes of the characteristics with the concentration u_m between x_1 and x_2 may be zero or negative if Q_{u0} is high and Q_u low, *i.e.*, u_{m0} lies at or to the right of u^M.) The underflow concentration changes immediately from the initial value $u_{u0} = 7{\cdot}96$ to the new value $u_u = 8{\cdot}89$. There is an expansion wave at the bottom below the line of continuity $x_3 = f'(u_{M0})t + D$, along which the concentration is u_{M0}. The line x_1 is a contact discontinuity with the speed

$$x_1'(t) = S_f(u_{m0}, u_{M0}) = S_f(u_{m0}, u_{m0}^*) = f'(u_{M0}),$$

since $u_m(Q_u)^* = u_M(Q_u)$ for all values of Q_u ([2, Lemma 2.2]); see the long-dashed line in Figure 7. Hence, x_1 and x_3 are parallel straight lines. The discontinuities satisfy

$$\begin{aligned} x_1(t) &= f'(u_{M0})t + x_{sb0}, && 0 < t < t_1, \\ x_2(t) &= S_f(u_{m0}, u_m)t, && 0 < t < t_1, \\ x_4(t) &= S_f(u_m, u_{M0})t + x_1(t_1), && t_1 < t < t_2, \end{aligned}$$

where

$$t_1 = \frac{x_{sb0}}{S_f(u_{m0}, u_m) - f'(u_{M0})}, \qquad t_2 = \frac{D - x_1(t_1)}{S_f(u_m, u_{M0}) - f'(u_{M0})}.$$

The example data we use here give $t_1 \approx 29$ min and $t_2 \approx 3{\cdot}6$ h. There is an expansion wave at the bottom and x_5 approaches the final SBL x_{sb} asymptotically, since the concentration below the SBL approaches u_M asymptotically.

Because of the monotonicity property of $\tilde{u}_u(u_f, s)$, defined by (2), the new underflow concentration satisfies

$$u_u = \begin{cases} \tilde{u}_u(u_f, s) > \tilde{u}_u(u_{f0}, s_0) = u_{u0}, & s > \bar{q}_u u_{max}, \\ u_{u0} = u_{max} & s \leq \bar{q}_u u_{max}. \end{cases}$$

The mass in the settler is unchanged. This is because of the immediate change to the new constant underflow concentration by Condition Γ. The outgoing flux $= Q_u u_u / A = f(u_M) =$

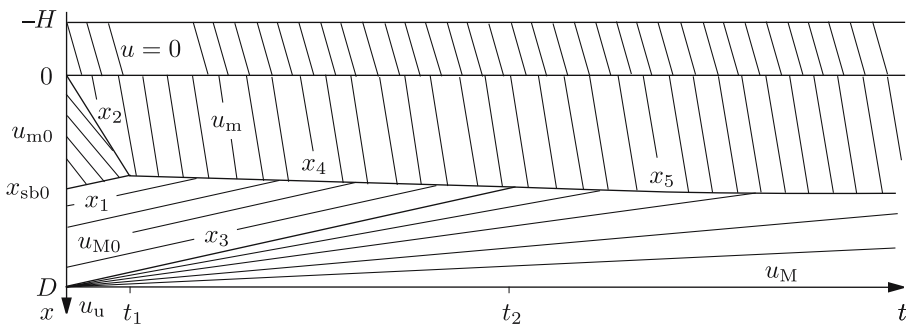

Figure 8. Solution of a response to DCL1 as $(u_f, s) \in \mathcal{U}_1(Q_{u0}) \cap \ell_2(Q_u)$.

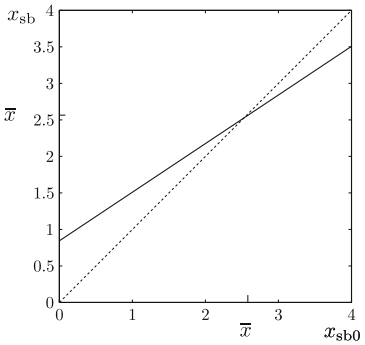

Figure 9. The solid line shows the relation (6); $x_{sb} = 0{\cdot}67x_{sb0} + 0{\cdot}84$ m. For example, $x_{sb0} = 2$ m gives $x_{sb} = 2{\cdot}18$ m, cf. Figure 10. The fixed point under the control action is $\bar{x} = 2{\cdot}53$ m.

$s =$ incoming flux. Equating the expression for the mass in the settler at $t = 0$, (5), and its analogue as $t \to \infty$, we get the following linear relationship between the new location of the SBL and the initial one (see Figure 9):

$$x_{sb} = \frac{x_{sb0}(u_{M0} - u_{m0}) + D(u_M - u_{M0})}{u_M - u_m}. \tag{6}$$

The properties

$$x_{sb} \to D\frac{u_M - u_{M0}}{u_M - u_m} > 0 \quad \text{as } x_{sb0} \to 0,$$
$$x_{sb} \to D\frac{u_M - u_{m0}}{u_M - u_m} < D \quad \text{as } x_{sb0} \to D,$$

imply, firstly, that there is a unique level, a fixed point of (6),

$$\bar{x} \equiv \frac{D}{1 + \frac{u_{m0} - u_m}{u_M - u_{M0}}},$$

which satisfies $x_{sb0} = \bar{x} = x_{sb}$ and, secondly, that *the control action has a stabilizing effect on the SBL* in the sense that x_{sb} lies closer to $\bar{x}$ than x_{sb0} does; *cf.* Figure 9. If $s_0 \le \bar{q}_u u_{max}$, then $x_{sb} = 0$. Compare the numerical values in the text above with the numerical simulation in Figure 10.

6.3. $(u_f, s) \in \mathcal{U}_1(Q_{u0}) \cap \Lambda_3$

Note that the solution in Figure 8 does not depend on the new value of the feed concentration u_f. Following the control strategy DCL1, we can find a value $Q_u < Q_{u0}$ such that $(u_f, s) \in \ell_3(Q_u)$. Then the solution is qualitatively the same as in the previous case $\mathcal{U}_1 \cap \Lambda_2$, but with f closer to f_0; see Figure 11 (left) and a simulation in Figure 12.

As a comparison we show in Figure 13 the solution when the slightly lower value $Q_u = \tilde{Q}_u = 3226$ is chosen according to DCL2, which implies $(u_f, s) = (7{\cdot}5, 9{\cdot}5) \in \mathcal{U}_1(Q_{u0}) \cap \ell_4(\tilde{Q}_u)$; see Figure 11 (right). There will not be any sludge blanket in the new steady state, which arises after a finite but long time. The solution will initially be as in Figure 8 with the concentration u_m replaced by $u_1 \in (u_m, u_{m0})$, satisfying $s = f(u_1)$. Note that s is now slightly greater than $f(u_m) = f(u_M)$. There is a small expansion wave emanating from the bottom. Its slowest rising discontinuity carries the concentration $u_1^* \in (u_{M0}, u_M)$. After this has met the rising sludge blanket (*cf.* the discontinuity x_5 in Figure 8), the speed of the sludge blanket stays at the constant and slightly negative value $x_5'(t) = S_f(u_1, u_1^*) = f'(u_1^*)$. Hence, it rises slowly until

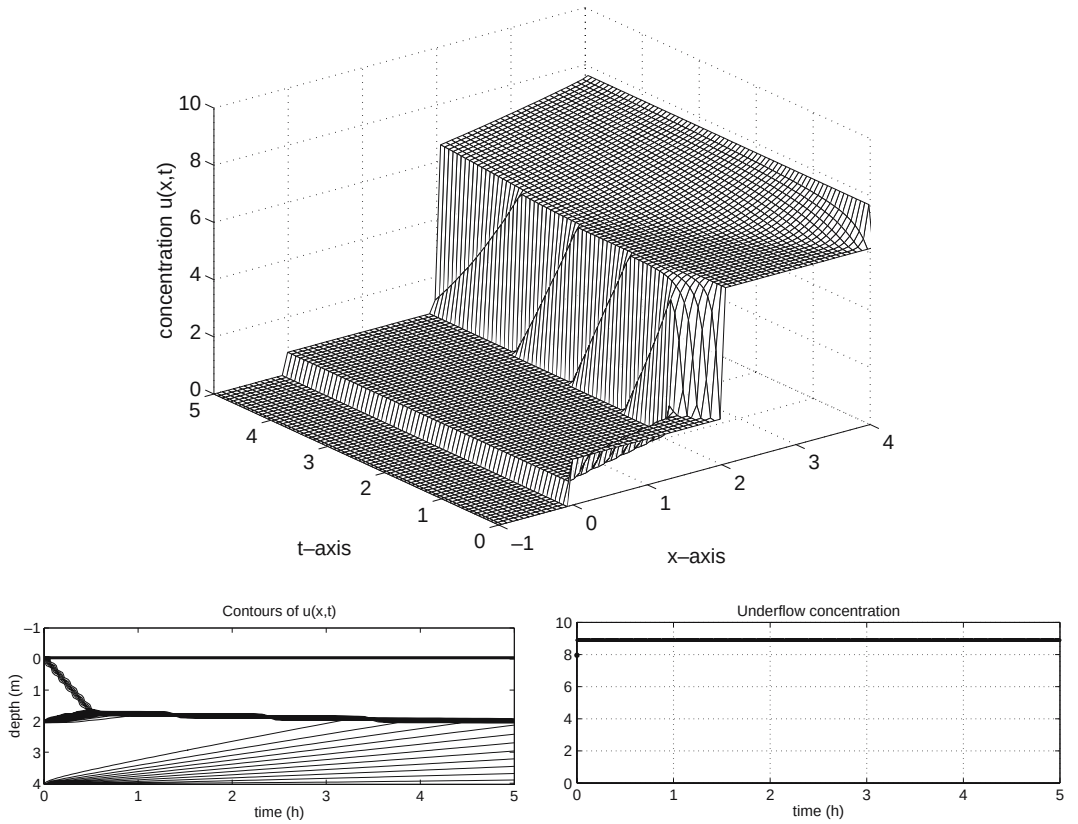

Figure 10. Numerical simulation of a response to DCL1 as $(u_f, s) = (2{\cdot}5, 6{\cdot}0) \in \mathcal{U}_1(Q_{u0}) \cap \ell_2(Q_u = 1908)$. Note the jump in the underflow concentration at $t = 0$.

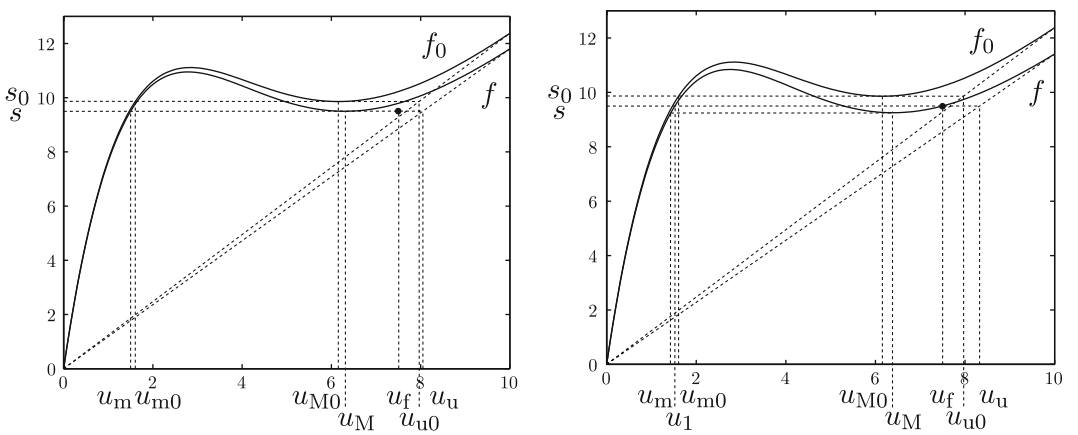

Figure 11. $(u_f, s) = (7{\cdot}5, 9{\cdot}5) \in \mathcal{U}_1(Q_{u0}) \cap \Lambda_3$. DCL1: $Q_u = \ell_3^{-1}(u_f, s) = 3337$ (left). DCL2: $Q_u = \ell_4^{-1}(u_f, s) = 3226$ (right).

it reaches the feed level. After that time point the new boundary concentration just below the feed level is u_f ($>u_M$) and this concentration is slowly spread all over the thickening zone. At this time point the underflow concentration makes a step increase from $f(u_M)/q_u$ to s/q_u and the new steady state begins.

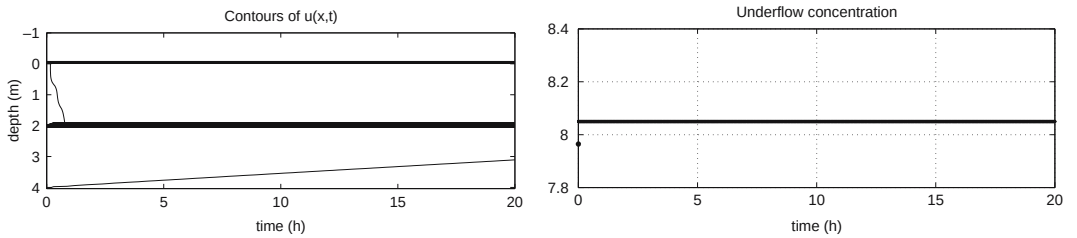

Figure 12. Numerical simulation of a response to DCL1; $(u_f, s) = (7{\cdot}5, 9{\cdot}5) \in \mathcal{U}_1(Q_{u0}) \cap \ell_3(Q_u = 3337)$. The settler is kept in optimal operation.

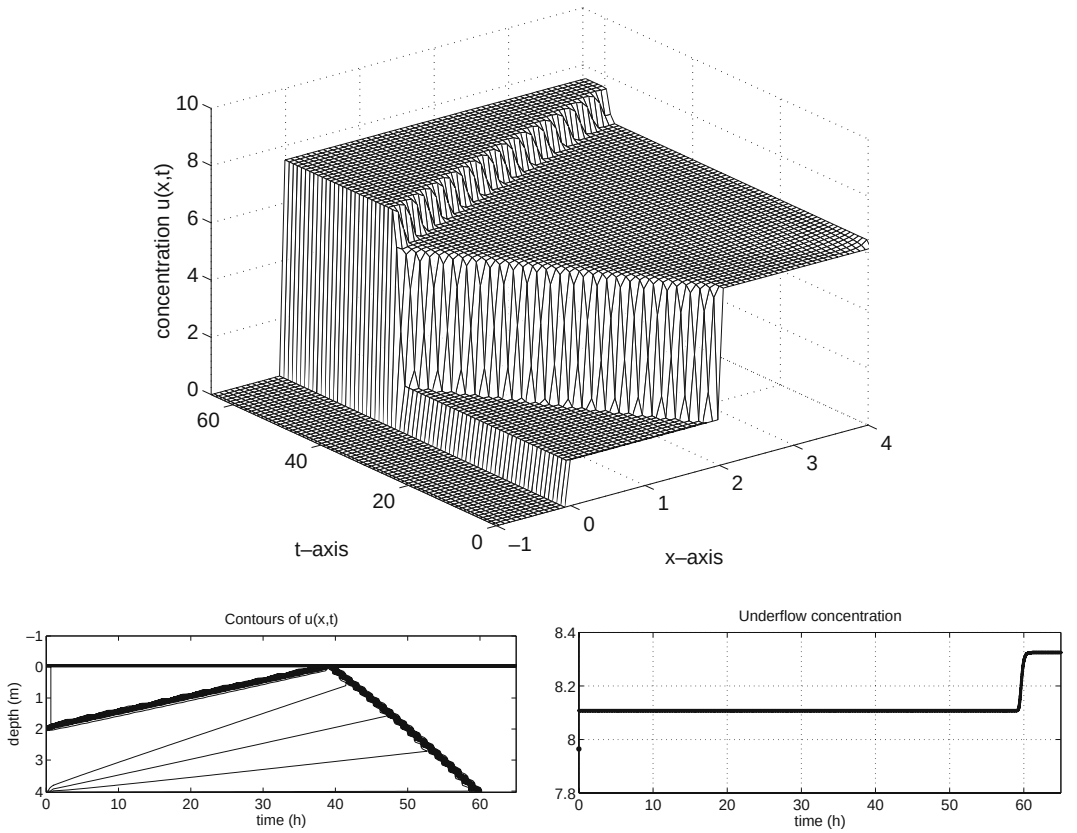

Figure 13. Numerical simulation of a response to DCL2; $(u_f, s) = (7{\cdot}5, 9{\cdot}5) \in \mathcal{U}_1(Q_{u0}) \cap \Lambda_3 \cap \ell_4(Q_u = 3226)$. Initially, the solution is similar to the one in Figure 12, however, with a rising SBL instead. Optimal operation is left at about 39 hours.

6.4. $(u_f, s) \in \big(\ell_1(Q_{u0}) \cup \mathcal{U}_1(Q_{u0})\big) \cap \Lambda_1$

The set is represented by a narrow strip in the control chart; see Figure 6. Choosing $Q_u = \tilde{Q}_u$ according to DCL1 = DCL2, we obtain a solution that initially (before t_2) looks like the one shown in Figure 8 with the concentration u_m replaced by u_f. Note that $s = f(u_f)$ is now less than $f(u_{M1})$, where u_{M1} is the new bottom concentration at $t = 0+$; see Figure 14. This implies that the discontinuity x_5, the SBL, has positive speed varying from $S_f(u_f, u_{M0})$ (during $t_1 < t \le t_2$) to the slightly lower value $S_f(u_f, u_{M1})$ as it reaches the bottom. At this time point the underflow concentration makes a step decrease from $f(u_{M1})/q_u$ to $f(u_f)/q_u = s/q_u$. A numerical simulation in the case $(u_f, s) = (1, 7{\cdot}5)$ and $\tilde{Q}_u = 2907$ is shown in Figure 15.

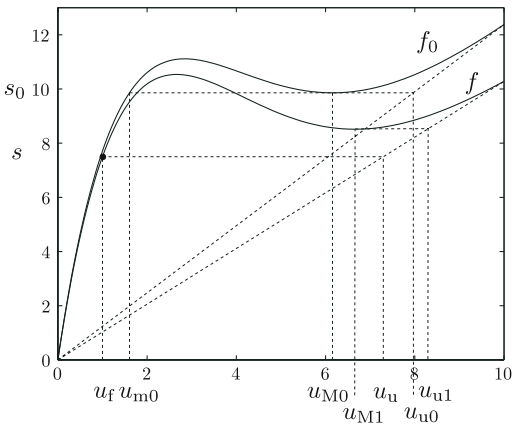

Figure 14. The feed point and fluxes in the case $(u_f, s) = (1, 7{\cdot}5) \in \mathcal{U}_1(Q_{u0}) \cap \ell_1(Q_u = 2907)$.

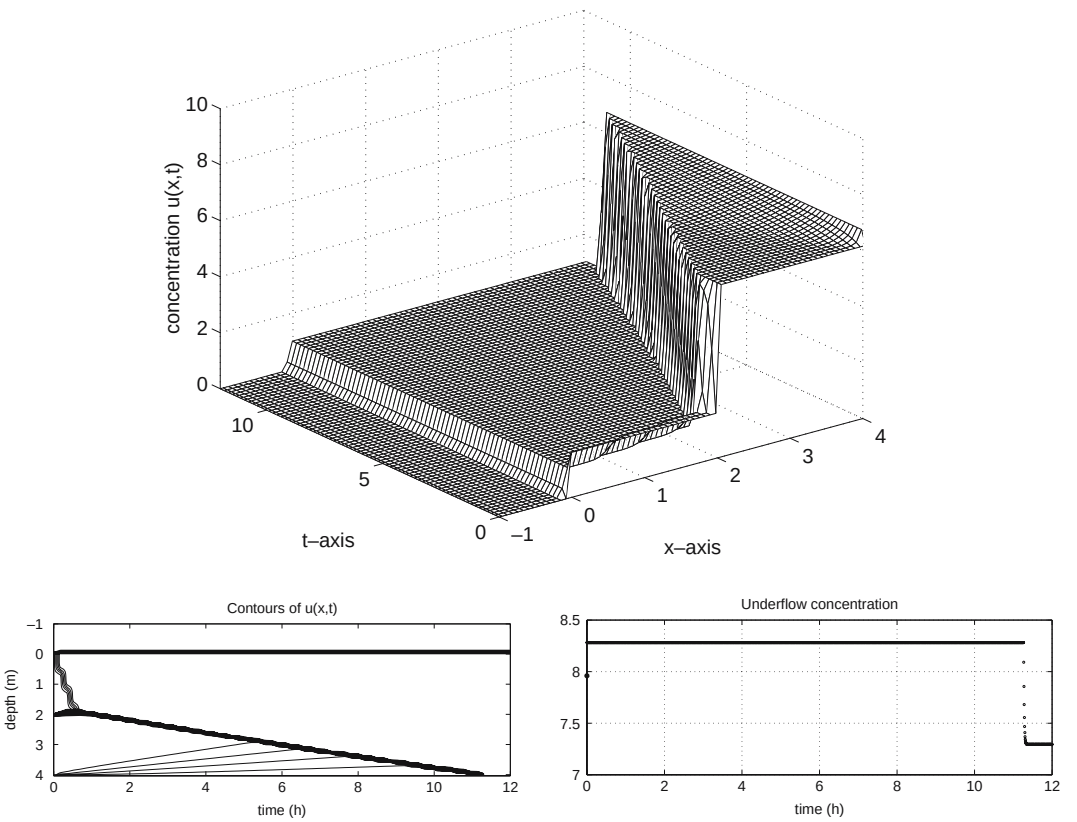

Figure 15. Numerical simulation of a response to DCL1 as $(u_f, s) = (1, 7{\cdot}5) \in \mathcal{U}_1(Q_{u0}) \cap \ell_1(\tilde{Q}_u = 2907)$. Note the jump in the underflow concentration at $t = 0$. Optimal operation is left at $t = 11{\cdot}6$ h.

6.5. $(u_f, s) \in \big(\mathcal{O}(Q_{u0}) \cup \ell_4(Q_{u0}) \cup \mathcal{U}_2(Q_{u0})\big) \cap (P \cup \Lambda_2 \cup \Lambda_3)$

For the numerical demonstration we assume that $(u_f, s) = (3, 11{\cdot}5) \in \mathcal{O}(Q_{u0}) \cap \Lambda_2$; see Figure 16. According to DCL1 we let, at $t = 0$, $Q_u = \ell_2^{-1}(u_f, s) = \tilde{Q}_u \approx 4298$ and hope that the settler stays in optimal operation. In fact, if the feed point were located in Λ_{3a}, we would obtain qualitatively the same solution when choosing $Q_u = \ell_3^{-1}(u_f, s)$. If $(u_f, s) \in \Lambda_{3b} \cup P_2$, then, with $Q_u = \tilde{Q}_u$, the solution is qualitatively the same as the one presented here, but

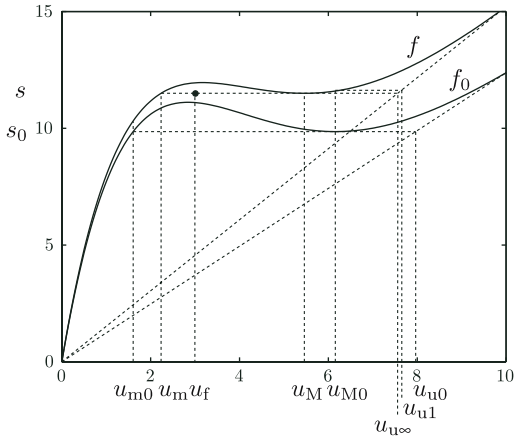

Figure 16. The feed point and flux functions in the case $(u_f, s) = (3, 11{\cdot}5) \in \mathcal{O}(Q_{u0}) \cap \ell_2(Q_u = 4298)$.

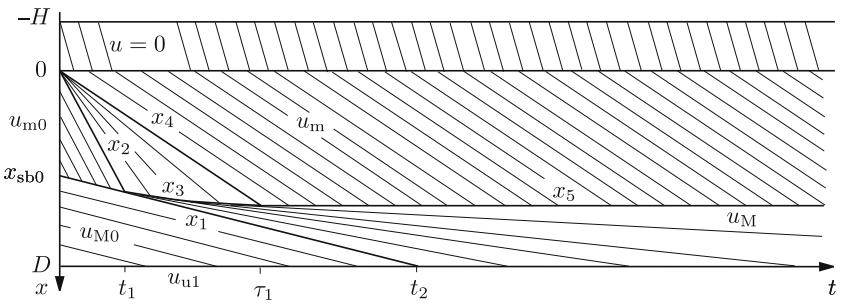

Figure 17. Solution of a response to DCL1 as $(u_f, s) \in \mathcal{O}(Q_{u0}) \cap \ell_2(Q_u)$. Note the jump in $u_u(t)$ at $t = 0$.

degenerate in the sense that $u_m = u_M = u_{infl}$. Furthermore, the settler leaves optimal operation directly since $Q_u \geq \bar{\bar{Q}}_u$.

We consider first the case when the initial SBL is not too close to the bottom; see Figure 17. Note that the characteristics below x_5 all emanate from the contact discontinuity x_3 (*cf.* [2, Equation (15)]). We have

$$\begin{aligned} x_1(t) &= S_f(u_{m0}, u_{M0})t + x_{sb0} = f'(u_{M0})t + x_{sb0}, && 0 < t < t_2, \\ x_2(t) &= f'(u_{m0})t, && 0 < t < t_1, \\ x_4(t) &= f'(u_m)t, && 0 < t < \tau_1, \end{aligned}$$

from which we obtain

$$t_1 = \frac{x_{sb0}}{f'(u_{m0}) - f'(u_{M0})}, \qquad t_2 = \frac{D - x_{sb0}}{f'(u_{M0})}.$$

The underflow concentration makes a jump at $t = 0$ down to u_{u1} and after $t = t_2$ it decreases continuously to its asymptotic value $u_{u\infty}$. The initial, intermediate and asymptotic underflow concentrations satisfy

$$\begin{aligned} u_{u0} &= \frac{f_0(u_{M0})}{q_{u0}} = u_{M0} + \frac{A f_b(u_{M0})}{Q_{u0}} > \\ u_{u1} &= \frac{f(u_{M0})}{q_u} = u_{M0} + \frac{A f_b(u_{M0})}{Q_u} > \\ u_{u\infty} &= \frac{f(u_M)}{q_u} = u_M + \frac{A f_b(u_M)}{Q_u}, \end{aligned}$$

where the first inequality follows directly from the fact that $Q_u > Q_{u0}$ and the second follows indirectly from this fact, since $u_M(Q_u)$ is a decreasing function of Q_u for $Q_u < \bar{\bar{Q}}_u$ ($\Leftrightarrow u_M > u_{infl}$) and $f_b(u)$ is decreasing for $u > u_{infl}$. The mass decreases according to

$$m(t) = \begin{cases} m_0 + t(As - Q_u u_{u1}), & 0 \le t \le t_2 \\ m_0 + t_2(As - Q_u u_{u1}) + \int_{t_2}^{t} \left(As - Q_u u_u(\tau)\right) d\tau, & t \ge t_2, \end{cases}$$

where we note that $As = Q_u u_{u\infty} < Q_u u_u(\tau)\ \forall \tau \ge t_2$.

Since the contact discontinuity $x_3(t)$ can only be obtained numerically generally, there is neither an explicit expression for τ_1 nor for the new SBL, $x_{sb} = x_5$. The latter constant lies between $x_1(t_1) = x_2(t_1)$ and the intersection of x_1 and a prolongation of x_4, which occurs at

$$\tau_2 \equiv \frac{x_{sb0}}{f'(u_m) - f'(u_{M0})} > \tau_1. \tag{7}$$

Hence, we have the following estimate for the new SBL:

$$\frac{x_{sb0}}{1 - f'(u_{M0})/f'(u_{m0})} = x_1(t_1) < x_{sb} < x_1(\tau_2) = \frac{x_{sb0}}{1 - f'(u_{M0})/f'(u_m)}. \tag{8}$$

The asymptotic relationship between the mass and the new sludge blanket level, $m_\infty = A\left(u_M D - x_{sb}(u_M - u_m)\right)$, can then be used to estimate the new mass.

Numerical values corresponding to Figure 16 and obtained by the formulae above are

$u_f = 3\,kg/m^3$	$u_{M0} = 6{\cdot}16\,kg/m^3$	$t_1 = 0{\cdot}8\,h$	
$s = 11{\cdot}5\,kg/(m^2h)$	$u_M = 5{\cdot}46\,kg/m^3$	$t_2 = 7{\cdot}1\,h$	
$Q_{u0} = 3500\,m^3/h$	$u_{u0} = 7{\cdot}96\,kg/m^3$	$\tau_2 = 2{\cdot}3\,h$	
$Q_u = 4298\,m^3/h$	$u_{u1} = 7{\cdot}63\,kg/m^3$	$2{\cdot}2\,m = 1{\cdot}1x_{sb0} < x_{sb}$	
$u_{m0} = 1{\cdot}61\,kg/m^3$	$u_{u\infty} = 7{\cdot}56\,kg/m^3$	$< 1{\cdot}3x_{sb0} = 2{\cdot}7\,m,$	Equation (8)
$u_m = 2{\cdot}23\,kg/m^3$			

A numerical simulation is shown in Figure 18.

Suppose now that the initial sludge blanket is located near the bottom, such that SBL reaches the bottom before τ_1. Then lower concentrations than u_m reach the bottom and Condition Γ implies that the underflow concentration will be lower than the previous value $u_{u\infty}$ shown in Figure 16. In such a case the solution can be described (qualitatively) by cutting off the solution shown in Figure 17 at a level between $x = x_{sb0}$ and $x = x_5$ and defining the cutting level as the new bottom level. The boundary concentrations at the bottom all imply, by [2, Equation (6)], that there is no wave (characteristic or discontinuity) emanating from the bottom upwards. To demonstrate this, we perform a simulation with the same data as above, except that we let $x_{sb0} = 3{\cdot}75$ m; see Figure 19. In this example the SBL reaches the bottom without any interaction with x_2. This implies that the bottom concentration is $u_D = u_{m0}$ and, by [2, Equation (6)] and (4), that the underflow concentration $f(u_{m0})/q_u = 6{\cdot}87$ kg/m^3 (at $t \approx 1$ h) is lower than the asymptotic value $u_{u\infty} = 7{\cdot}56$ kg/m^3.

In the latter circumstances the settler cannot be kept in optimal operation by performing this type of direct control action. Since we cannot compute x_3 or τ_1 exactly, a safe margin above the bottom for the SBL is obtained if the initial one satisfies

$$x_1(\tau_2) \le D \quad \Longleftrightarrow \quad x_{sb0} \le \left(1 - \frac{f'(u_{M0})}{f'(u_m)}\right) D, \tag{9}$$

which yields $x_{sb0} \le 0{\cdot}76D = 3{\cdot}04$ m with the present data. Numerical simulations yield that the actual boundary depth is 3·32 m.

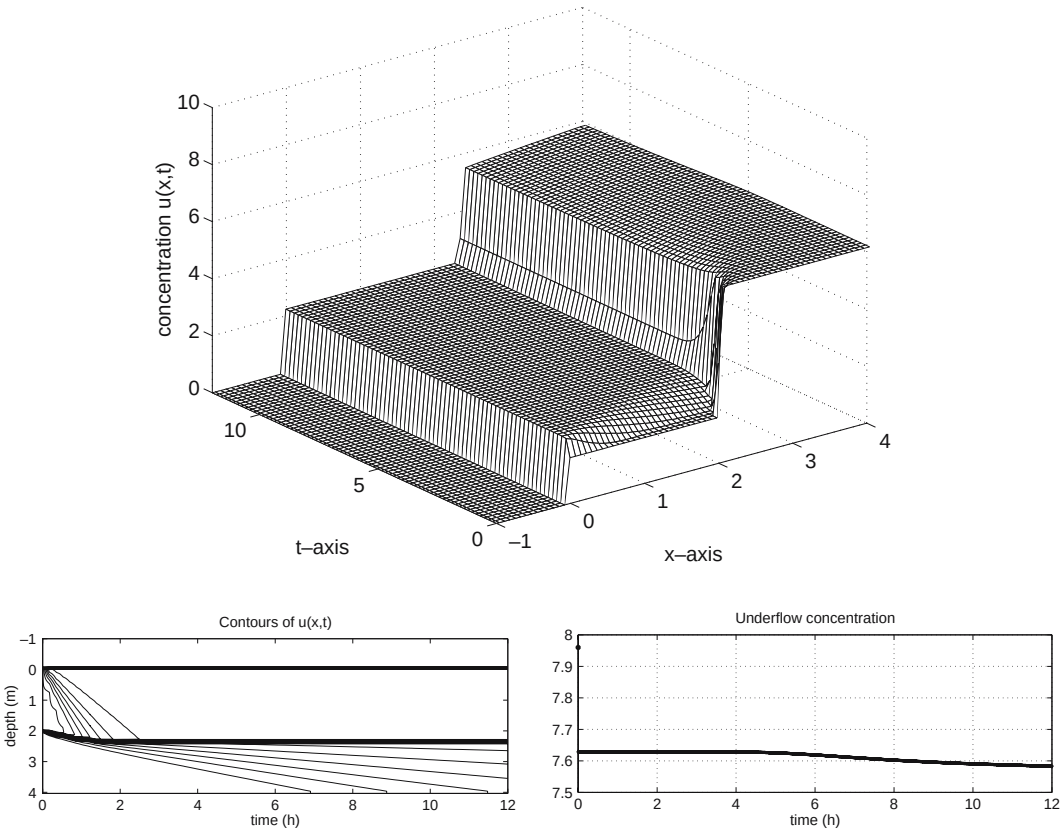

Figure 18. Numerical simulation of a response to DCL1 as $(u_f, s) \in \mathcal{O}(Q_{u0}) \cap \ell_2(Q_u)$. Note the jump in $u_u(t)$ at $t = 0$.

Consider DCL2, which differs from DCL1 only if $(u_f, s) \in \Lambda_3$ in the sense that Q_u is then set to the slightly lower value $\tilde{Q}_u$ such that $(u_f, s) \in \ell_4(\tilde{Q}_u)$. This means that the settler is critically loaded, but optimal operation cannot be maintained in the new steady state. The solution is then as the one in [2, case $\mathcal{U}_{2a}$, $s < f(u_0^M)$]. (If $(u_f, s) \in \mathcal{U}_{2a}$, *i.e.*, the feed point lies below the graph of f, then Q_u is actually slightly less than Q_{u0}.) If the SBL lies close to the bottom, DCL2 may be advantageous over DCL1 since optimal operation may not be left after a short time. However, in such a case it is easier to postpone any control action; see Section 7.

6.6. $(u_f, s) \in \mathcal{O}(Q_{u0}) \cap \Lambda_1$

Strategy DCL1 (= DCL2 = DCL3) means that $Q_u = \tilde{Q}_u > Q_{u0}$ is chosen such that $(u_f, s) \in \ell_1(Q_u)$. Suppose first that $Q_u < \bar{\bar{Q}}_u$. We obtain a solution that differs only slightly from the one in Figure 17. Compared to Figure 16 the feed point is now located on the graph of f to the left of u_m. The underflow concentration jumps directly down to $u_{u1} = f(u_{M0})/q_u$. The concentration on the right of x_4 is $u_f < u_m$ and $s = f(u_f) < f(u_m) = f(u_M)$ holds. (Note that s may be less or greater than s_0.) This implies that $u_f^* > u_M$ and the discontinuity x_5 has the positive speed $x_5'(t) = S_f(u_f, u_f^*) = f'(u_f^*)$. Hence, x_5 will reach the bottom at a finite time point, at which the underflow concentration makes a jump down to $u_{u\infty} = f(u_f)/q_u = s/q_u$. A numerical simulation in the case $(u_f, s) = (1{\cdot}8, 11{\cdot}0)$ is shown in Figure 20.

If $Q_u \geq \bar{\bar{Q}}_u$, the solution will qualitatively be the same with $u_m = u_M = u_{infl}$, however, optimal operation is left immediately by definition.

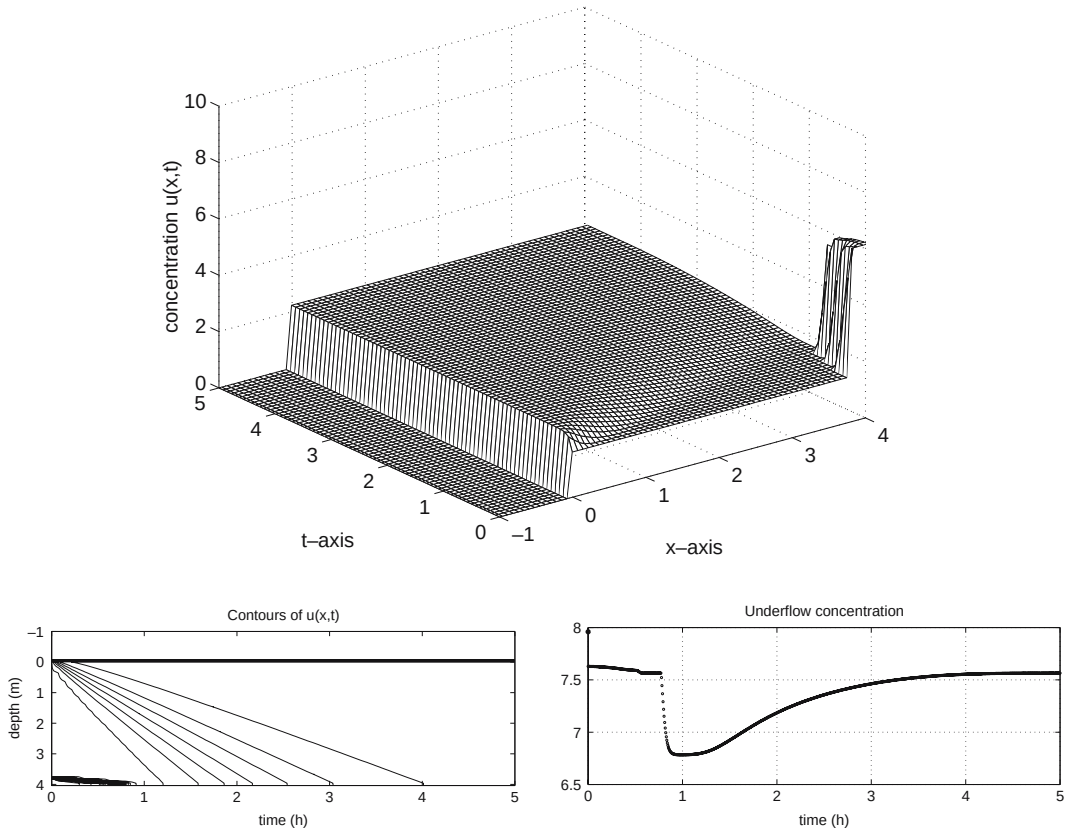

Figure 19. Numerical simulation of a response to DCL1 as $(u_f, s) \in \mathcal{O}(Q_{u0}) \cap \ell_2(Q_u)$ and with an initial sludge blanket near the bottom. Note the dip in the underflow concentration as the SBL reaches the bottom.

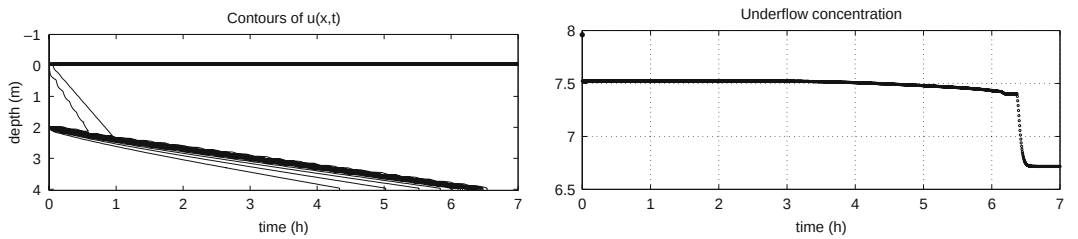

Figure 20. Numerical simulation of a response to DCL1 as $(u_f, s) = (1{\cdot}8, 11{\cdot}0) \in \mathcal{O}(Q_{u0}) \cap \ell_1(Q_u)$ with $Q_u < \overline{\overline{Q}}$. Optimal operation is left after 6·5 h.

6.7. $(u_f, s) \in \Lambda'_a$

To maintain optimal operation as long as possible, the best remedy is to increase the control variable as much as possible, *i.e.*, to set $Q_u = Q_f \Leftrightarrow Q_e = 0$. This is strategy DCL1. Then we obtain the slowest possible rising SBL; see the simulation in Figure 21.

There will not be any sludge blanket in the new steady state, which arises after a finite time. The solution is similar to the one constructed in [2, Figure 21], however, with a sinking SBL before t_1 (as in Figure 17) and with u_2 replaced by u_f as the new concentration in the thickening zone. The boundary concentration below the feed inlet is not u_m but higher. Since $s \leq f(u^M)$ (definition of Λ'_a) the initial boundary concentration below the feed level is u_1, defined by $s = f(u_1)$ and $u_m < u_1 \leq u^M$, *cf.* in [2, Figure 20 (left)]. (Note that on the boundary

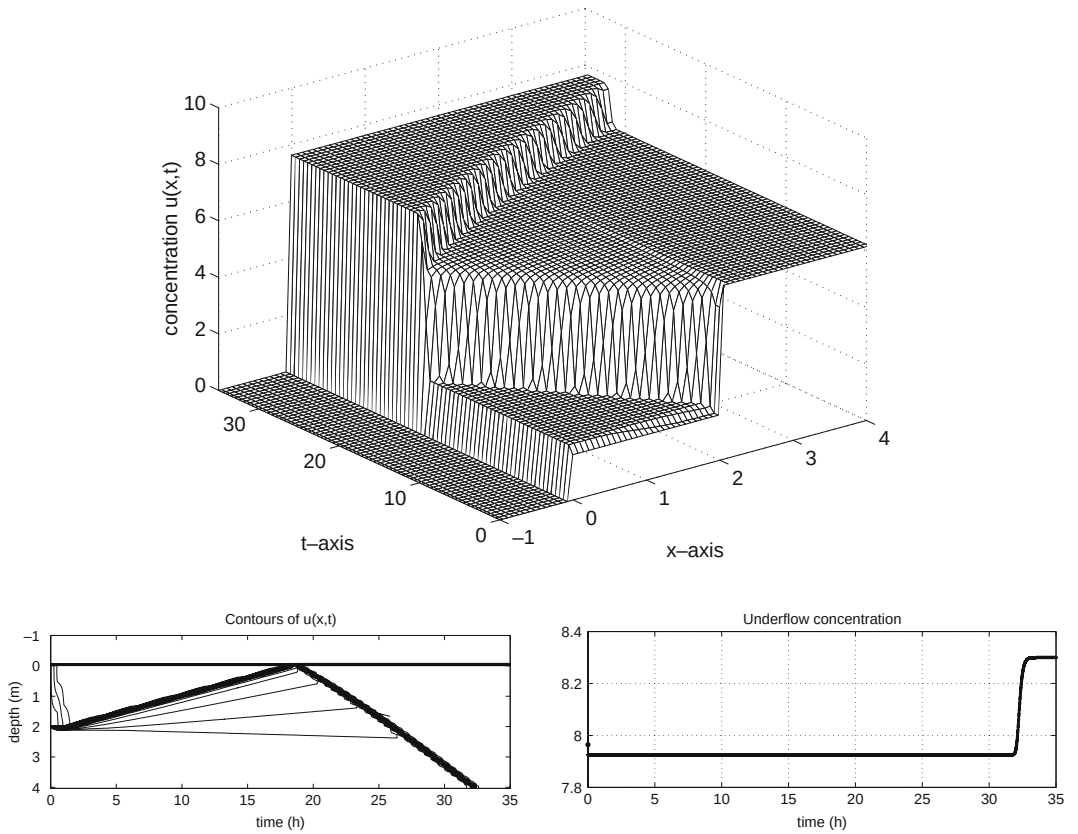

Figure 21. Numerical simulation of a response to DCL1 as $(u_f, s) = (8{\cdot}3, 10{\cdot}5) \in \Lambda'_a \cap \mathcal{U}_2(Q_{u0} = 3500)$ with $Q_u = Q_f = 3577\ m^3/h$. The pure liquid in the clarification zone is still ($Q_e = 0$). Optimal operation is left after 18 h. The settler is slightly underloaded and after $t \approx 33$ h $u_u = u_f$ holds.

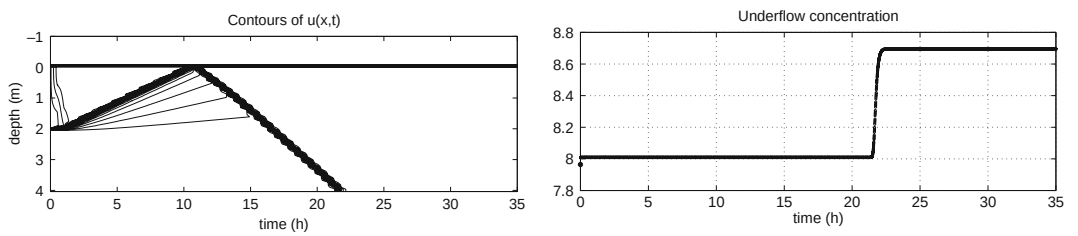

Figure 22. Numerical simulation of a response to strategy DCL2 as $(u_f, s) = (8{\cdot}3, 10{\cdot}5) \in \Lambda'_a \cap \mathcal{U}_2(Q_{u0} = 3500) \cap \ell_4(\tilde{Q}_u = 3414)$. Optimal operation is left after 11 h. In the new steady state the settler is critically loaded with $u_u = 8{\cdot}7\ kg/m^3$.

between Λ'_a and Λ'_b, $s = f(u^M) \Leftrightarrow u_1 = u^M$ holds and the initial expansion wave from the feed level reaches up to the feed level.) The rising sludge blanket has the negative speed $S_f(u_1, u_1^*)$. After it has reached the feed level (at $t \approx 18$ in Figure 21) the new boundary concentration below the feed level is $u_2 > u_{M0}$ ([2, Figure 20 (right)]), and this is eventually spread all over the thickening zone.

As a comparison, we show in Figure 22 the simulation for the case when strategy DCL2 is invoked: the control variable is set to $Q_u = \ell_4^{-1}(u_f, s) = \tilde{Q}_u = 3414$. Clearly, optimal operation is left earlier than in Figure 21.

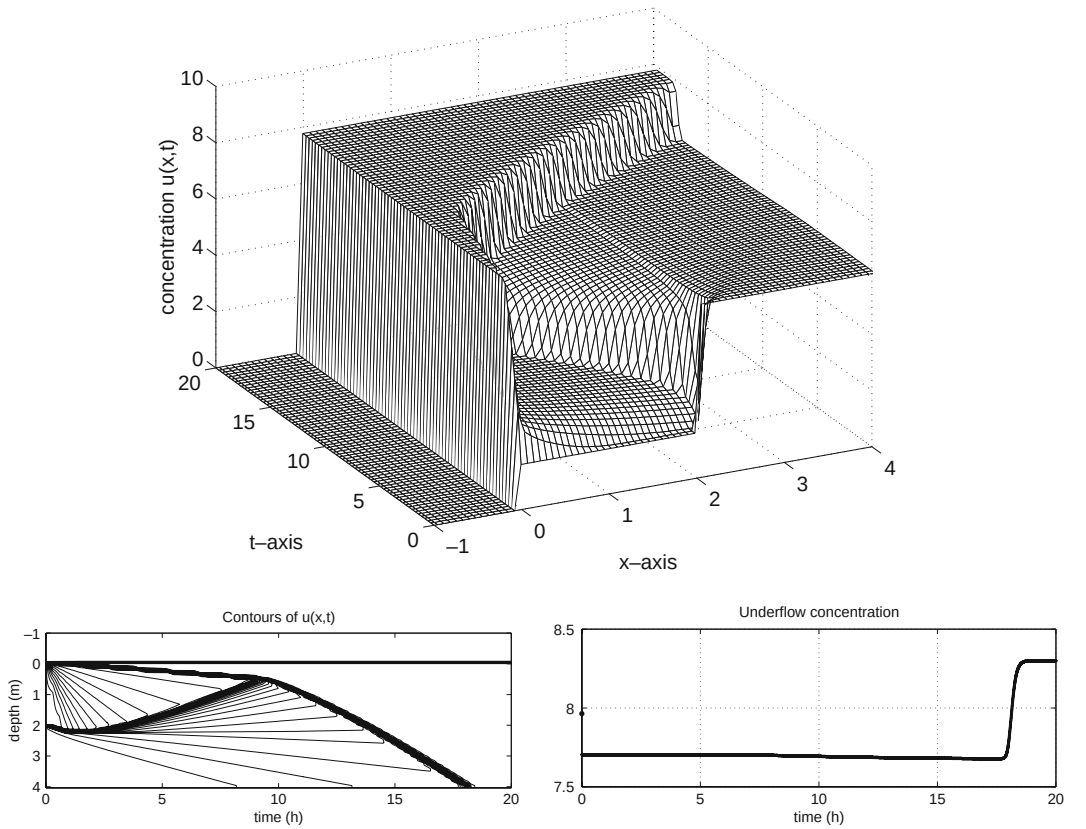

Figure 23. Numerical simulation of a response to DCL1 as $(u_f, s) = (8{\cdot}3, 12{\cdot}0) \in \Lambda'_b \cap \mathcal{O}(Q_{u0})$ and $Q_u = Q_f = 4088$ m^3/h. Note that the new underflow concentration, after 18 h, is $u_u = u_f = 8{\cdot}3$ kg/m^3.

6.8. $(u_f, s) \in \Lambda'_b$

By analogy with Section 6.7 the best remedy (to keep optimal operation as long as possible) is to let $Q_u = Q_f$, which corresponds to DCL1 = DCL2 = DCL3. Since $s > f(u^M)$, the new boundary concentration below the feed level is the high concentration $u_f > u_{infl}$ directly, *cf.* [2, Figure 23]. Optimal operation is therefore left immediately. The solution is demonstrated by the numerical simulation in Figure 23. Compare with the solution in [2, Figure 25].

7. Optimal control strategies of step inputs

7.1. Operating chart for optimal control of step inputs

Given a settler in optimal operation in steady state and a step input, we have in [2] seen the response without any control action, and in Section 6 the response to a direct control action. With this information we can obtain optimal control strategies with respect to the control objectives CO1–CO3 defined in Section 4. Therefore, we combine the information in the operating chart for direct control of step responses in Figure 6 with the operating chart for step responses and the safe and dangerous regions; see Figure 24 here and [2, Theorem 4.1]. Since the settler is not in optimal operation when $Q_u \geq \bar{\bar{Q}}_u$, see for example Section 6.6, we have to divide Λ_1 into two disjoint subsets, by analogy with the division of Λ_3 (see (3)):

$$\Lambda_{1a} = \Lambda_1 \cap \left\{(u, y) : y < f_b(u) + \bar{\bar{q}}_u u\right\} \quad \text{and} \quad \Lambda_{1b} = \Lambda_1 \setminus \Lambda_{1a}.$$

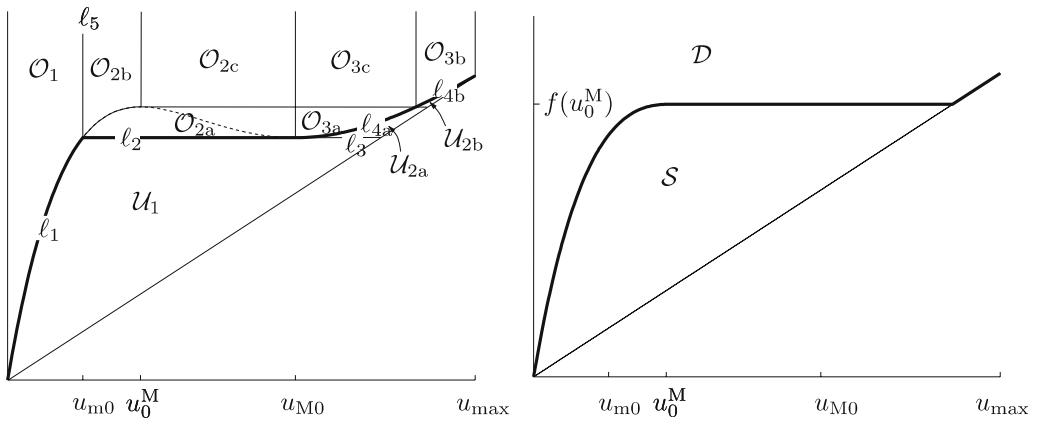

Figure 24. Operating charts from [2] shown with the initial value Q_{u0}. *Left:* Operating chart for step responses from optimal operation. *Right:* The 'dangerous' and 'safe' regions of the operating chart corresponding to whether optimal operation is left immediately or not after a step input. Referring to the control objects in Section 4 note that $L_3 = \partial\mathcal{S} \cap \partial\mathcal{D}$.

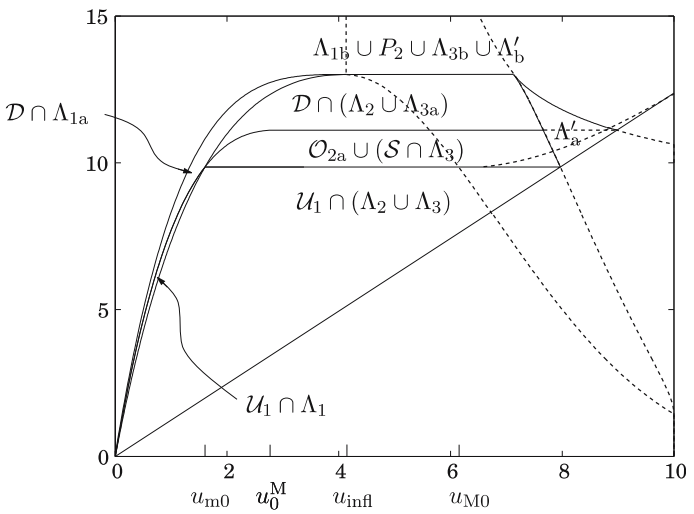

Figure 25. Operating chart for optimal control of step inputs. The regions are shown by solid lines. The sets refer to the initial value Q_{u0}, *i.e.*, $\mathcal{D} \equiv \mathcal{D}(Q_{u0})$ etc. Given a step change with (u_f, s) in a region, the optimal control strategies are shown in Table 2.

The resulting operating chart is shown in Figure 25 and in Table 2 we give an overview of the optimal control strategies. For CO2 and CO3 a lower bound u_u^{min} on the underflow concentration is prescribed. It is reasonable to assume that $u_u^{min} \le u_{u0}$ holds. Unless otherwise stated, we therefore assume that $u_u^{min} = u_{u0}$ holds as the worst case. In the following sections we comment upon the optimal strategies in Table 2 for each region.

7.2. $(u_f, s) \in \big(\ell_1(Q_{u0}) \cup \mathcal{U}_1(Q_{u0})\big) \cap \Lambda_1$

Without any control action the sludge blanket will decrease and after a finite time reach the bottom, see [2, Sections 4.2 and 4.4]. Note that DCL1 = DCL2 (Q_u is decreased to $\tilde{Q}_u$). This control action results in the slowest possible decrease of the SBL and implies that CO1 is fulfilled. A critically loaded settler is obtained as shown in Section 6.4. Since Q_u is decreased,

Table 2. Survey of optimal strategies for control of step inputs. Each case should be read from the left to the right. 'Optimal operation maintained until' refers to the control action stated in the adjacent left column. 'Delayed' means that a single step-control action is performed at a later time point. PCC is specified in the text in each case.

Region in operating chart (Figure 25)	Optimal control action to meet CO1 and first action of CO2	Optimal operation maintained until	Second control action to meet CO2	Optimal control action to meet CO3	Optimal operation maintained until
$(\ell_1 \cup \mathcal{U}_1) \cap \Lambda_1$	DCL1	SBL meets bottom	PCC	PCC	third control action
$\mathcal{U}_1 \cap (P \cup \Lambda_2 \cup \Lambda_3)$	DCL1 or delayed L1	$t = \infty$	none	DCL1 or delayed L1	$t = \infty$
$\mathcal{O}_{2a} \cup (\mathcal{S} \cap \Lambda_3)$	DCL1 if (9) is true, else delayed L1	$t = \infty$	none	delayed L1	SBL meets feed level
$\mathcal{D} \cap (\Lambda_2 \cup \Lambda_{3a})$	(9) is true: DCL1	$t = \infty$ if (9) is true	none	PCC	$t = 0$ if $u_u^{\min} = u_0$
	(9) is false: DCL3. If SBL does not meet bottom, 2nd action to meet CO1: L1	SBL does not meet bottom: $t = \infty$	L1		
		SBL meets bottom	PCC		
Λ'_a	DCL1	SBL meets feed level	$Q_u = Q_{u0}$ if $(u_f, s) \in \mathcal{S}$, else L3	delayed L2	SBL meets feed level if $(u_f, s) \in \mathcal{S}$, else $t = 0$
$\mathcal{D} \cap \Lambda_{1a}$	DCL1	SBL meets bottom	PCC	delayed L1	$t = 0$
$\Lambda_{1b} \cup P_2 \cup \Lambda_{3b} \cup \Lambda'_b$	CO1: DCL1; CO2: see CO3	$t = 0$	none	delayed L1	$t = 0$

$u_u(t) = u_{u0} = u_u^{\min}$ holds until the SBL reaches the bottom, *i.e.*, as long as optimal operation is maintained. Therefore, CO2 and CO3 are equivalent. After the SBL has reached the bottom, the underflow concentration drops below u_{u0}. To fulfil CO2, Theorem 4.1 yields that Q_u should be lowered further to $Q_u^{\max 1}$ just before the SBL reaches the bottom. Then there will be a rising discontinuity in the clarification zone. Just before this one reaches the effluent level, Q_u should be set back to $\tilde{Q}_u$ to keep $u_e = 0$ and satisfy CO2 and CO3. This is demonstrated in Figure 26.

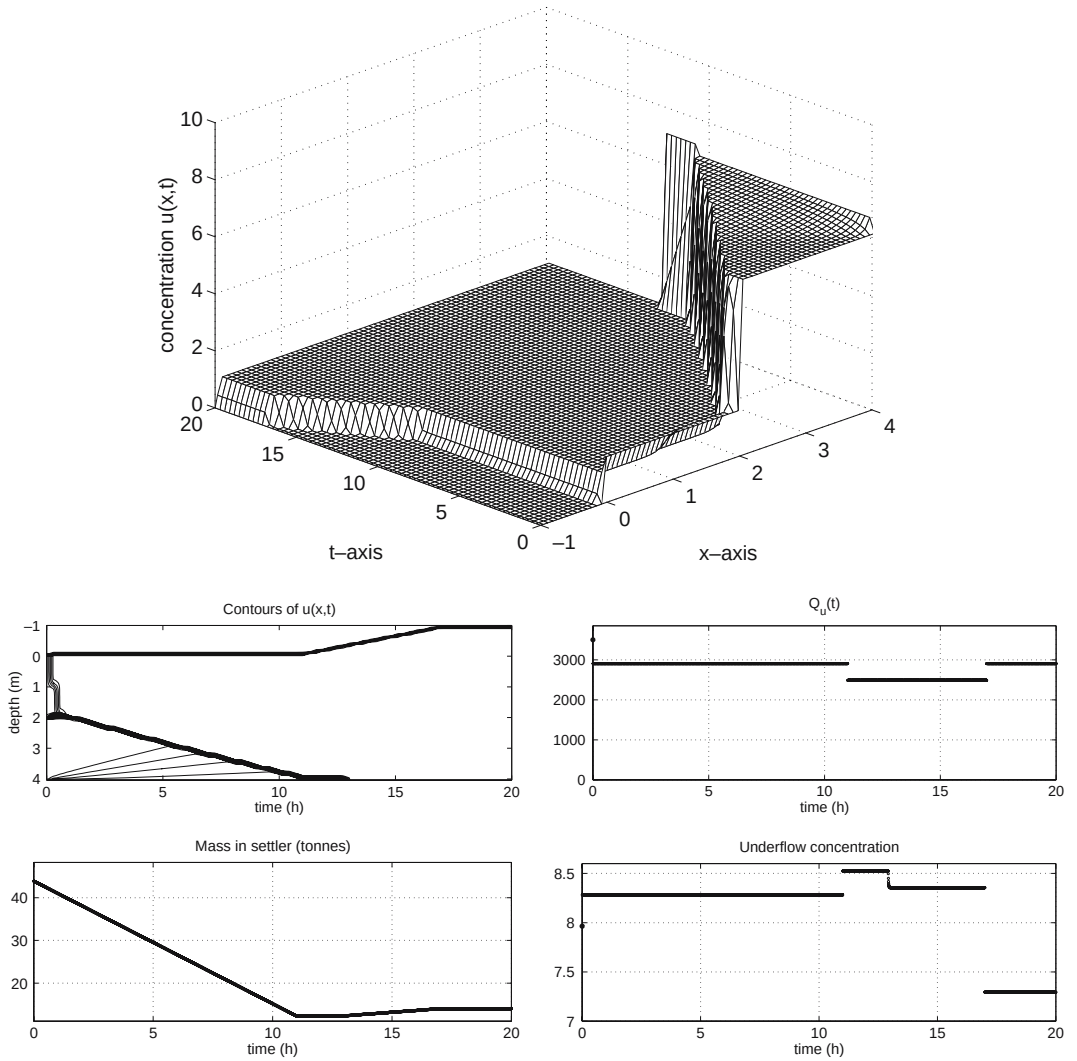

Figure 26. Optimal PCC with respect to CO2 and CO3 as $(u_f, s) = (1, 7{\cdot}5) \in \mathcal{U}_1(Q_{u0}) \cap \Lambda_1$. Optimal operation is left at $t = 11$ h but $u_u(t) \geq u_{u0} = 7{\cdot}96$ kg/m^3 until $t = 17$ h instead of $t \approx 11{\cdot}2$ h as in DCL1; see Figure 15.

7.3. $(u_f, s) \in \mathcal{U}_1(Q_{u0}) \cap (P \cup \Lambda_2 \cup \Lambda_3)$

In Sections 6.2 and 6.3 we have seen that DCL1 has a stabilizing effect on the SBL, the mass is unchanged and the underflow concentration makes a step increase directly and then stays constant. Since $(u_f, s) \in \mathcal{S}$, there is an option to wait a while before a control action is made; see the step response in [2, Section 4.2], which shows that the underflow concentration is constant and the mass and the SBL decreases. Performing L1 at a time point t_c before the SBL reaches the bottom (which occurs at $t = T_u = (m - m_0)/(s - s_0)$; see [2]), we obtain a new steady state with a mass and SBL, both of which are lower the closer t_c is to T_u. The mass in the settler can actually be set to a fixed value below m_0 and above ADu_m depending on the choice of t_c. This is demonstrated with a simulation in Figure 27, in which the initial data and step change are the same as in Section 6.2. To ensure that the new steady state has a SBL above the bottom, t_c cannot be too near T_u, because of the transient that appears after t_c. Finally, we conclude that all these control actions satisfy CO1, CO2 and CO3.

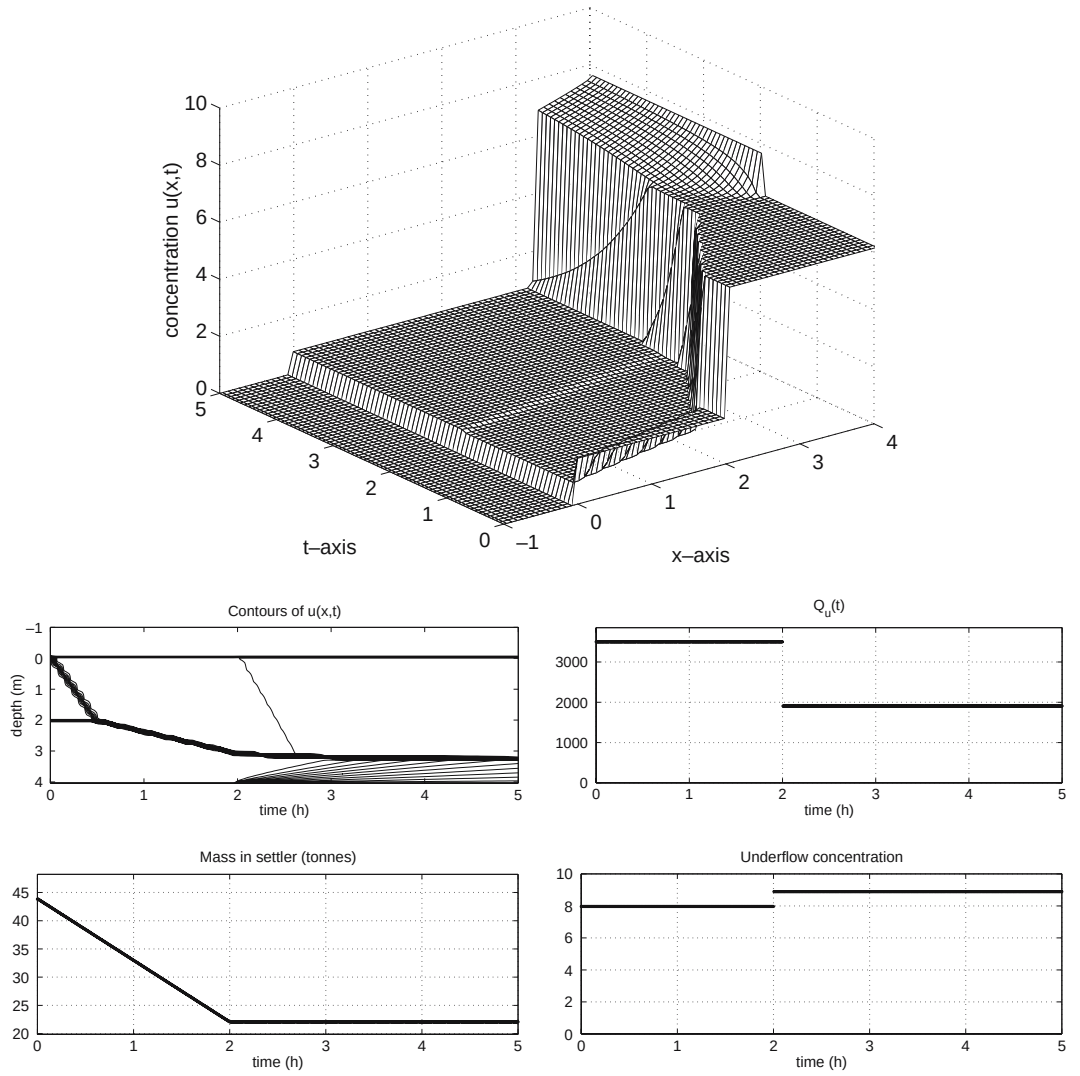

Figure 27. Optimal control with respect to CO1, CO2 and CO3 as $(u_f, s) = (2{\cdot}5, 6{\cdot}0) \in \mathcal{U}_1(Q_{u0}) \cap \Lambda_2$. A control action, $Q_u = \tilde{Q}_u = 1908$, is performed at $t = t_c = 2$ h instead of $t = 0$ as in Figure 10.

7.4. $(u_f, s) \in \mathcal{O}_{2a}(Q_{u0}) \cup \big(\mathcal{S}(Q_{u0}) \cap \Lambda_3\big)$

If (9) is satisfied, CO1 is fulfilled by DCL1 as shown in Section 6.5. In that section we have also seen that, if the sludge blanket lies close to the bottom, DCL1 may imply that optimal operation is left after a short time. This is because Q_u has been increased too much. DCL2 may be (only in the case $(u_f, s) \in \Lambda_3$) slightly more advantageous but it is easier to wait with any control action. Even for a higher-located sludge blanket a step increase in Q_u may violate CO2 and CO3, since the underflow concentration decreases directly with a step. Waiting a while before performing the control action resolves this. During the step response the mass increases initially and the SBL rises after a while, see [2, Sections 4.7–4.10]. The solution is qualitatively the same in all those cases up to $t = T_{cl}$, which is the time point when particles start to enter the clarification zone. Performing the control action L1 at $t_c \in (0, T_{cl})$, the settler remains in optimal operation. Hence both CO1 and CO2 are fulfilled. Assume that the initial data and step input are the same as in [2, Section 4.7.1]: $Q_{u0} = 2000$, $s_0 = 6{\cdot}25$, $u_f = 5{\cdot}52$,

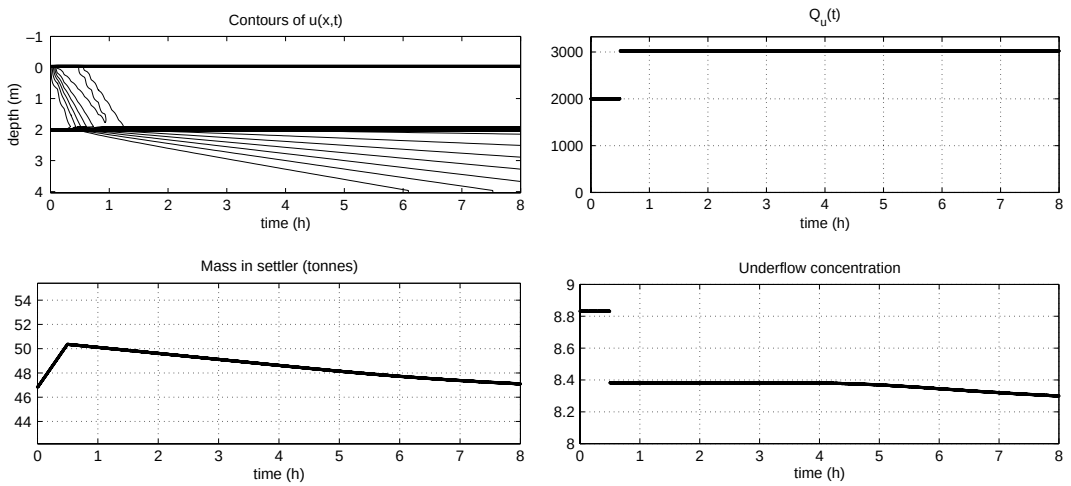

Figure 28. Optimal control with respect to CO1 and CO2 (optimal operation is maintained) as $(u_f, s) = (5{\cdot}52, 8{\cdot}79) \in \mathcal{O}_{2a}(Q_{u0} = 2000)$. Q_u is set to $\tilde{Q}_u = L_1^{-1}(u_f, s) = 3023$ at $t_c = 0{\cdot}5$ h. Note that after 8 hours the mass and SBL are approximately the same as the initial values.

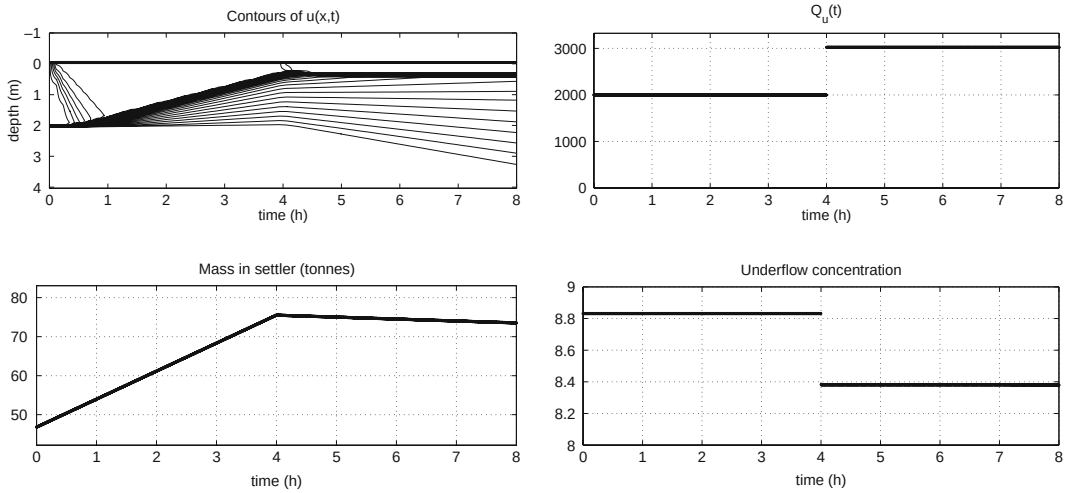

Figure 29. The same data as in Figure 28 but with $t_c = 4$ h.

$s = 8{\cdot}79$. Then $\tilde{Q}_u \approx 3023$ m^3/h and simulations in the cases $t_c = 0{\cdot}5$ h and $t_c = 4$ h $< T_{cl} \approx 4{\cdot}8$ h are shown in Figures 28 and 29, respectively.

Since there is a drop in the underflow concentration at $t = t_c$, CO3 is fulfilled by performing the L1-step just before the discontinuity reaches the effluent level; see Figure 30.

7.5. $(u_f, s) \in \mathcal{D}(Q_{u0}) \cap (\Lambda_2 \cup \Lambda_{3a})$

Since $(u_f, s) \in \mathcal{D}$ we know from [2, Theorem 4.1] that optimal operation is left immediately unless a direct control action (Q_u is increased) is performed. In Section 6.5 we have seen that if (9) is satisfied, DCL1 implies that optimal operation is maintained and an estimation of the depth of the new SBL is given by (8). Any increase in Q_u from Q_{u0} will imply a decreasing SBL initially. Hence, if SBL is close to the bottom, a high value of Q_u is needed. The highest possible value (to maintain optimal operation) corresponds to a feed point on the boundary between $\mathcal{D}$ and $\mathcal{S}$, *i.e.*, $Q_u = L_3^{-1}(u_f, s)$. Hence, strategy DCL3 will either maintain optimal operation or imply the slowest sinking SBL possible to satisfy CO1. This is demonstrated in

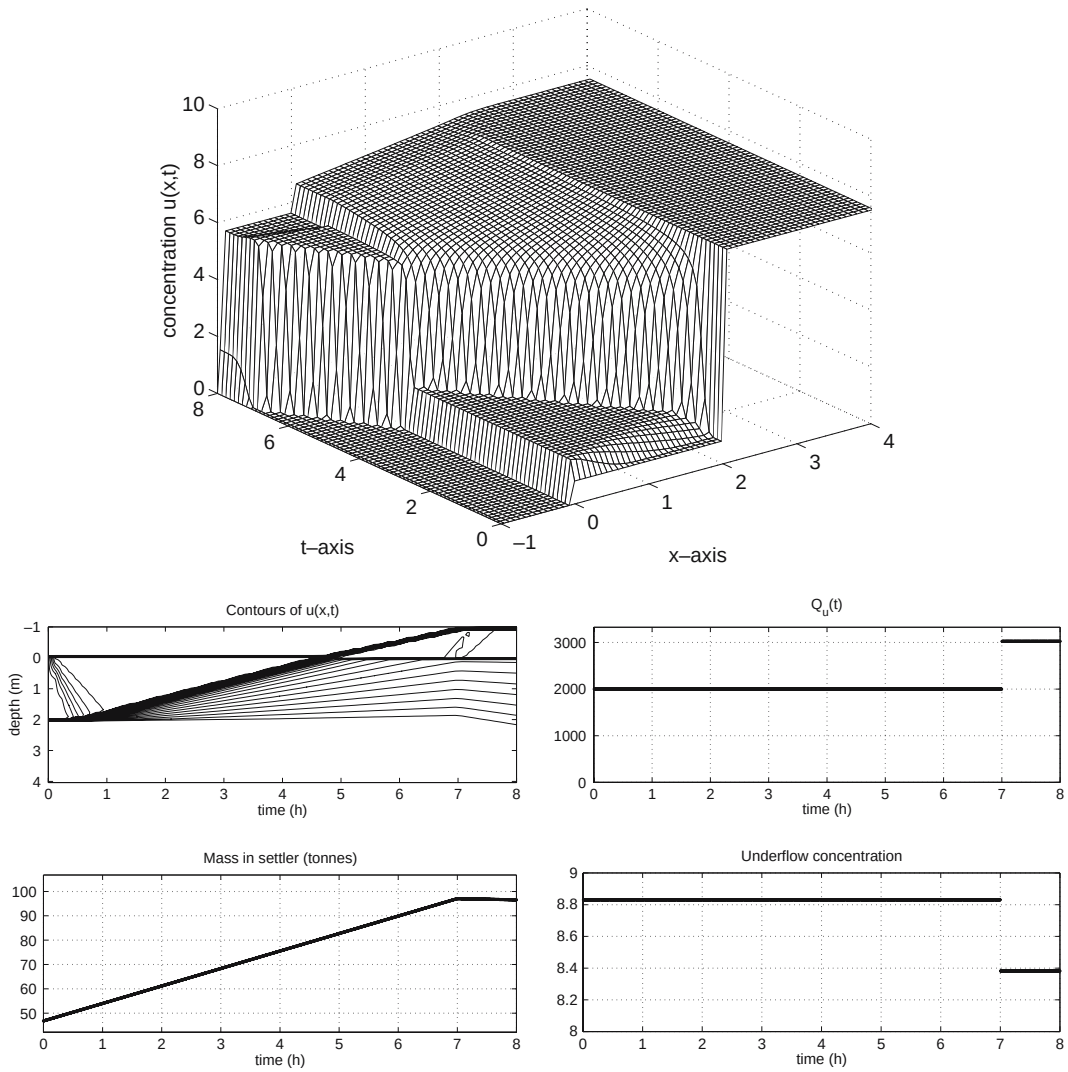

Figure 30. Initial data as in Figures 28 and 29. Optimal control with respect to CO3 with the control action L1 at $t_c = 7$ h. Note that $u_e = 0$ for $t > 0$. The discontinuity in the clarification zone stays just below the top of the settler. In the new steady state the particles in the clarification zone is thus still.

Figure 31, where the initial data are the same as in Figure 19. If the initial depth of the SBL is slightly less, optimal operation can be maintained substantially longer by performing an L1-step at a later time point; see Figure 32.

To satisfy CO2 Theorem 4.1 yields that Q_u should be decreased to $Q_u^{max1} = Q_{u0}$ as the SBL reaches the bottom. Then $u_u = u_{u0} = u_u^{min}$, but there will be a rising discontinuity in the clarification zone. Since the situation is similar to satisfying CO3, see below, we do not show any solution in this case.

From the proof of Theorem 4.1 we can also conclude that any step increase to $Q_u > Q_{u0}$ will directly result in a step decrease in the underflow concentration. Hence, for any $(u_f, s) \in \mathcal{D}$, there is no control action that can result in optimal operation subject to $u_u \geq u_u^{min}$. Optimal operation must be left directly and hence CO2 = CO3. To satisfy this objective, the first control action, which is L3, has to be delayed until just before the rising discontinuity in the clarification zone reaches the effluent level; see Figure 33. After the discontinuity in the

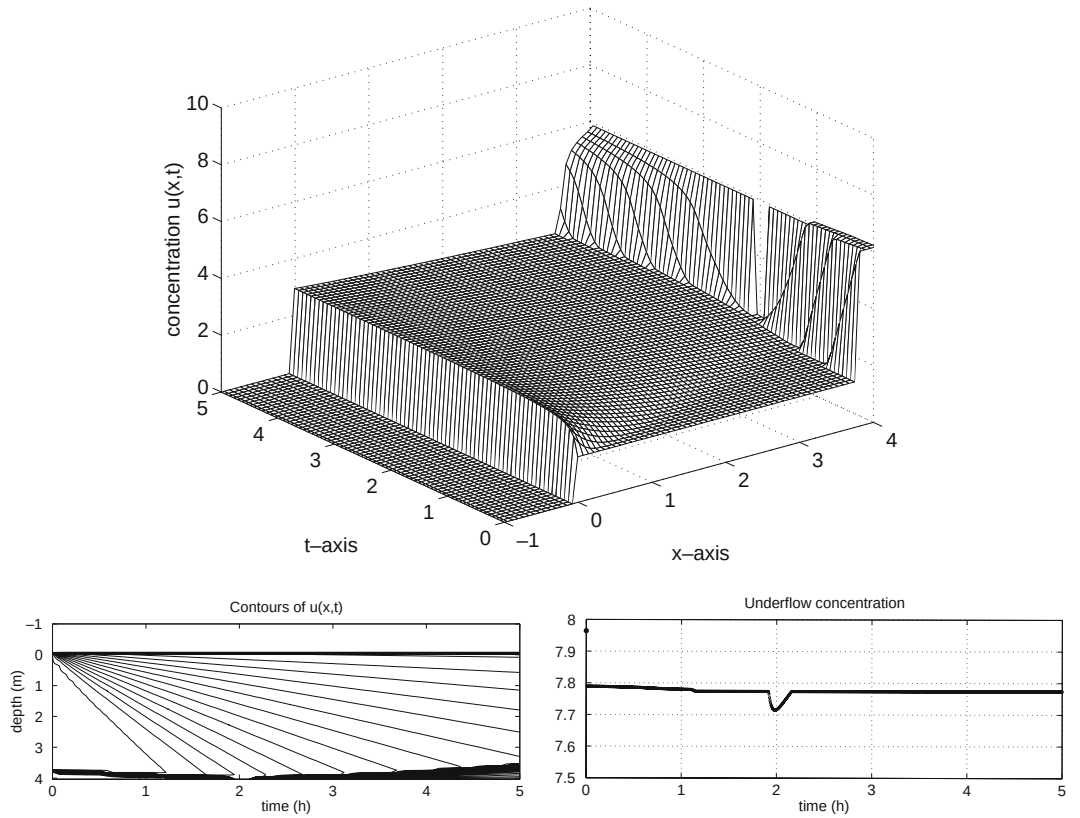

Figure 31. DCL3 with $Q_u = 3876$ in order to satisfy CO1 as $(u_f, s) = (3, 11{\cdot}5) \in \mathcal{D}(Q_{u0} = 3500) \cap \Lambda_2$ and $x_{sb0} = 3{\cdot}75$ m; *cf.* Figure 19. Optimal operation is left during a short period around $t \approx 2$ h as the SBL reaches the bottom.

thickening zone has reached the feed level, there is a small rising wave in the clarification zone, which will yield particles in the effluent unless L1 is invoked.

Now suppose that $u_u^{\min}$ is lower than the initial value, say 7·7 kg/m^3. Then CO3 can be fulfilled with optimal operation until the SBL moves up into the clarification zone. Just before it reaches the effluent level, the control variable is set according to L1; see Figure 34.

7.6. $(u_f, s) \in \Lambda'_a$

From the solutions presented in [2, Sections 4.8.1 and 4.8.3] and in Section 6.7 here we can conclude that DCL1 is the optimal control action to satisfy CO1. This means that Q_u is increased to its physically maximal value for the given feed point, *i.e.*, $Q_u = Q_f$. This implies that the underflow concentration makes a step decrease directly. Hence, if $u_u^{\min} = u_{u0}$, then CO2 is not satisfied. The initial underflow concentration can be brought back by letting $Q_u = Q_{u0}$ when the SBL reaches the feed level, provided $(u_f, s) \in \mathcal{S}(Q_{u0})$. This is demonstrated in Figure 35, in which we use the same numerical data as in Section 6.7. If $(u_f, s) \in \mathcal{D}(Q_{u0})$, Q_u cannot be lowered to Q_{u0}. The lowest value required to maintain optimal operation is obtained with action L3 just before the SBL reaches the feed level *or* just before the rising discontinuity in the clarification zone reaches the effluent level, whichever occurs first. The solution is not substantially different from the one in Figure 35.

In order to satisfy CO3, Q_u must not be increased because of the constraint $u_u(t) \geq u_u^{\min}$. Hence, if $(u_f, s) \in \mathcal{S} \cap \big(\mathcal{U}(Q_{u0}) \cup \ell_4\big)$, the control variable should not be changed at all. If

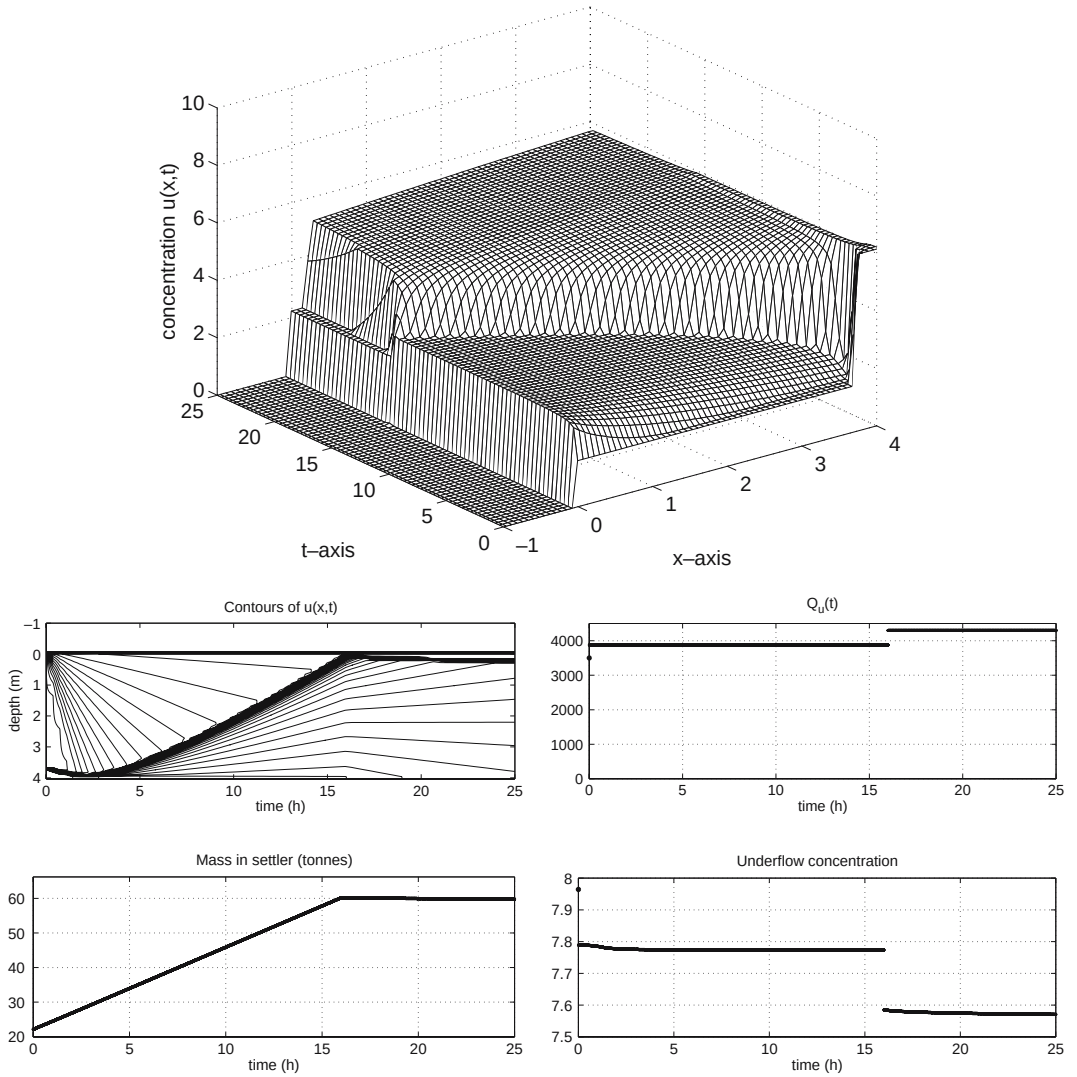

Figure 32. Optimal control with respect to CO1 and CO2 as $(u_f, s) = (3, 11{\cdot}5) \in \mathcal{D}(Q_{u0} = 3500) \cap \Lambda_2$ and $x_{sb0} = 3{\cdot}70$ m. DCL3 is followed by an L1-step at $t = 16$ h.

$(u_f, s) \in \mathcal{S} \cap \mathcal{O}(Q_{u0})$, an L2-action is performed just before particles reach the effluent level to prevent an overflow, *cf.* Figure 30. If $(u_f, s) \in \mathcal{D}$, optimal operation and $u_u(t) \geq u_u^{min}$ cannot be satisfied together. Then CO3 is met by a delayed control action L2 just before overflow occurs; see Figure 36.

7.7. $(u_f, s) \in \mathcal{D}(Q_{u0}) \cap \Lambda_{1a}$

As presented in Section 6.6 DCL1 is the optimal control action to satisfy CO1; see Figure 20. Optimal operation is left as the SBL reaches the bottom. Optimal operation is inevitably left at this time point. To satisfy CO2, the SBL should be prevented from reaching the bottom by decreasing Q_u from its present value $\tilde{Q}_u$. This will yield a rising discontinuity in the clarification zone, of which the speed is greater the lower Q_u is. Since the concentrations above and below the sinking SBL are u_f and u_f^*, respectively, the SBL becomes stationary for the Q_u that satisfies $S_f(u_f, u_f^*) = 0 \Leftrightarrow f(u_f; Q_u) = f(u_f^*; Q_u) \Leftrightarrow Q_u = -Af_b'(u_f^*)$ (note that $Q_u < \bar{\bar{Q}}_u$

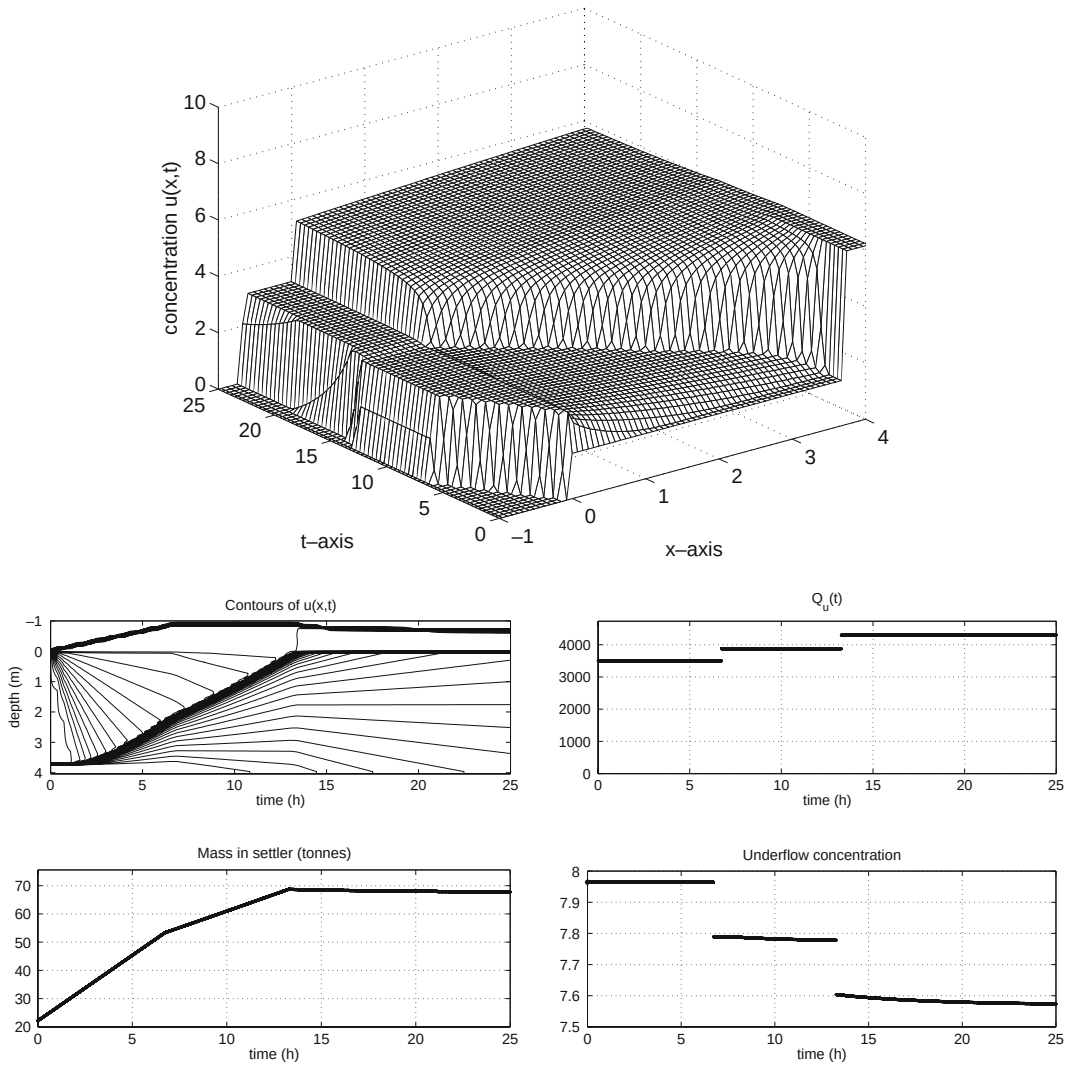

Figure 33. Optimal control with respect to CO2 and CO3 with $u_u^{\min} = u_{u0} = 7{\cdot}96$ kg/m^3 as $(u_f, s) = (3, 11{\cdot}5) \in \mathcal{D}(Q_{u0} = 3500) \cap \Lambda_2$ and $x_{sb0} = 3{\cdot}70$ m. Step-control actions with respect to L3 and L1 are performed at $t = 7$ h and $t = 13{\cdot}8$ h, respectively.

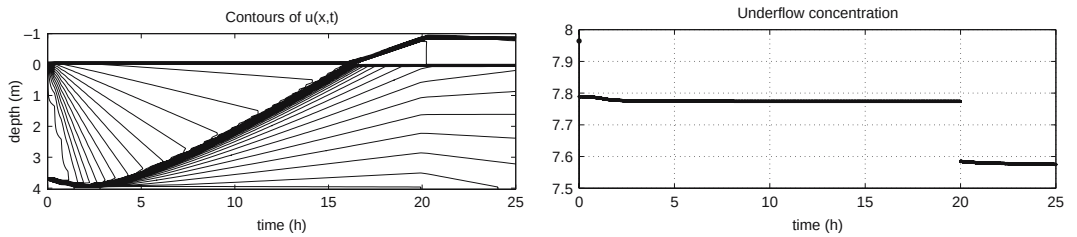

Figure 34. Optimal control with respect to CO3 with $u_u^{\min} = 7{\cdot}7$ kg/m^3 as $(u_f, s) = (3, 11{\cdot}5) \in \mathcal{D}(Q_{u0} = 3500) \cap \Lambda_2$ and $x_{sb0} = 3{\cdot}70$ m. DCL3 is followed by L1 at $t = 20$ h.

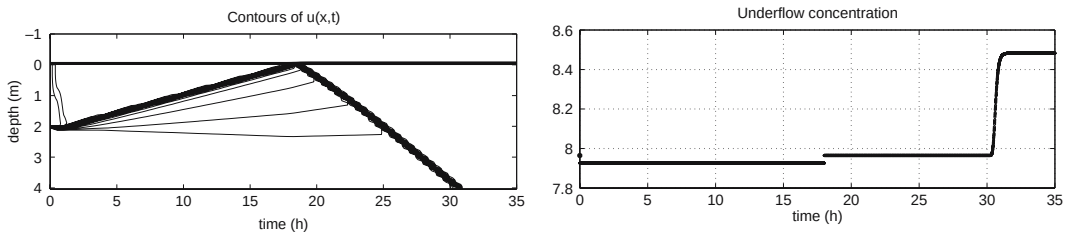

Figure 35. Optimal control with respect to CO2 as $(u_f, s) = (8{\cdot}3, 10{\cdot}5) \in \Lambda'_a \cap \mathcal{S}(Q_{u0} = 3500)$. DCL1 with $Q_u = Q_f = 3577$ is followed by setting $Q_u = Q_{u0}$ at $t = 18$ h.

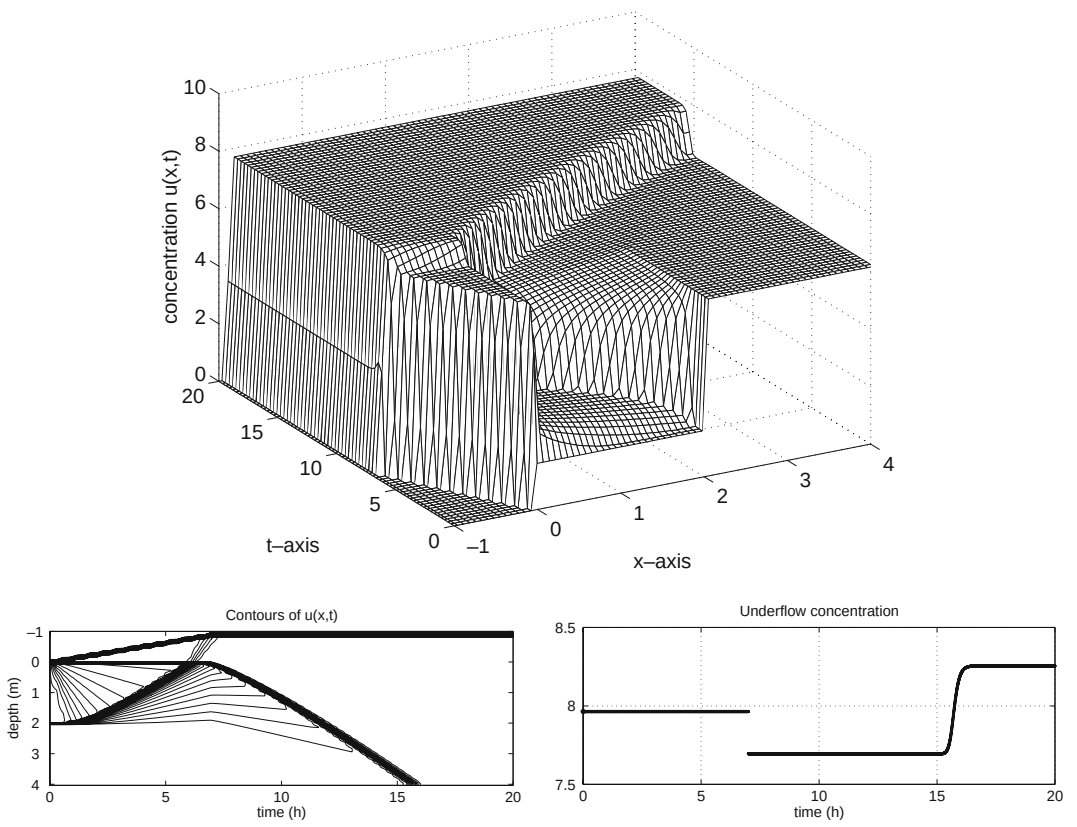

Figure 36. Optimal control with respect to CO3 as $(u_f, s) = (7{\cdot}7, 12) \in \Lambda'_a \cap \mathcal{D}(Q_{u0} = 3500)$. An L2-control action with $Q_u = \tilde{Q}_u = 4110$ is performed at $t = 7$ h.

by the definition of Λ_{1a}). Hence, set $Q_u = -Af'_b(u^*_f)$ just before the SBL reaches the bottom, see Figure 37, in which we have used the same initial data as in Figure 20. To keep $u_e = 0$ we set $Q_u = \tilde{Q}_u$ just before an overflow occurs. To satisfy CO3 with $u_u^{\min} = u_{u0}$ an L1-step should be performed just before the SBL reaches the effluent level; see Figure 38.

7.8. $(u_f, s) \in \Lambda_{1b} \cup P_2 \cup \Lambda_{3b} \cup \Lambda'_b$

This region is a subset of $\mathcal{D}(Q_{u0})$, which means that Q_u must be increased so that $(u_f, s) \in \mathcal{S}(Q_u)$, *i.e.*, the control action L1 = L2 = L3 should be performed to prevent particles from entering the clarification zone. This implies that $Q_u \geq \bar{\bar{Q}}_u$ if $(u_f, s) \in \Lambda_{1b} \cup P_2 \cup \Lambda_{3b}$ (see

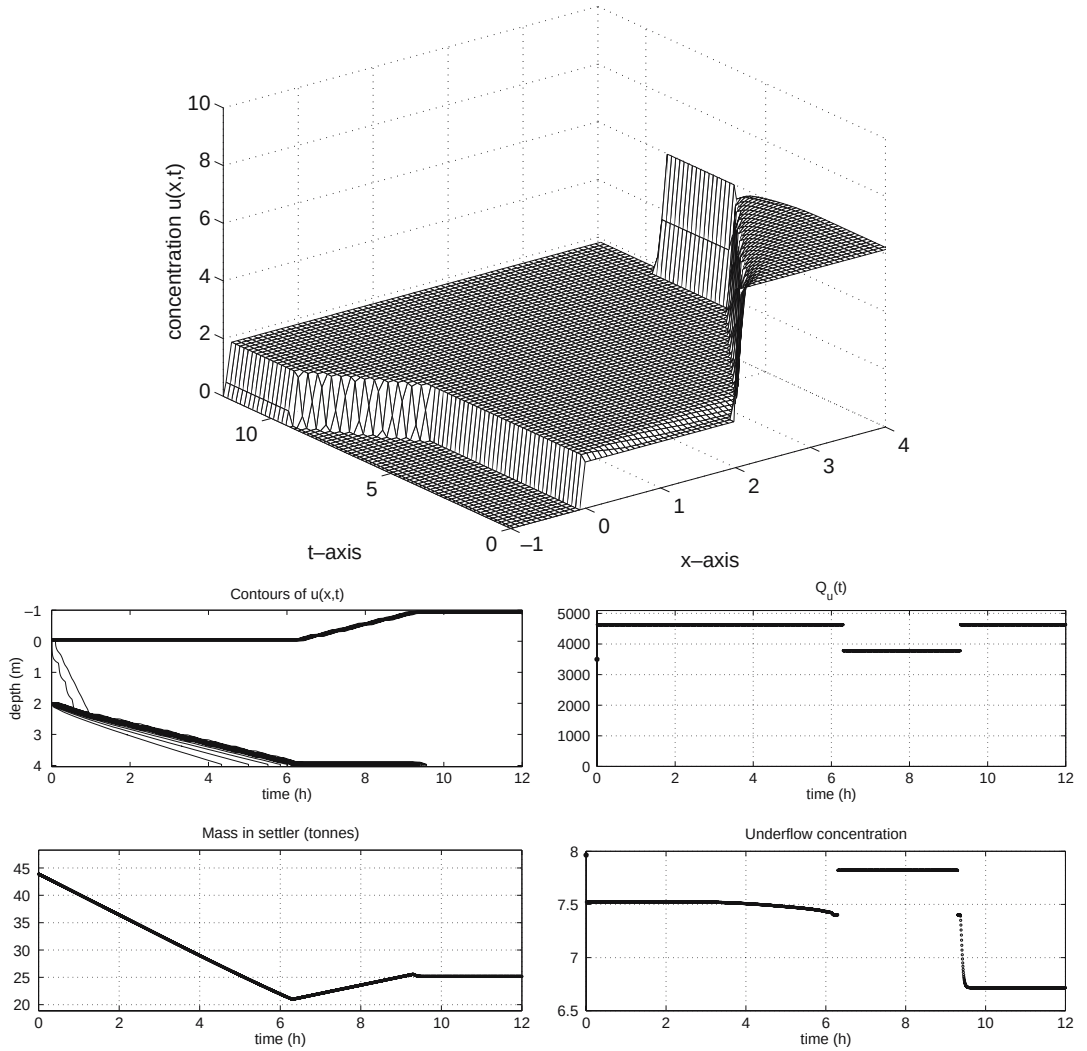

Figure 37. Optimal control with respect to CO2 as $(u_f, s) = (1{\cdot}8, 11{\cdot}0) \in \mathcal{D}(Q_{u0} = 3500) \cap \Lambda_{1a}$. DCL1 with $Q_u = \tilde{Q}_u = 4631$ is followed by $Q_u = -Af_b'(u_f^*) = 3781$ at $t = 6{\cdot}3$ h and $Q_u = \tilde{Q}_u$ at $t = 9{\cdot}3$ h.

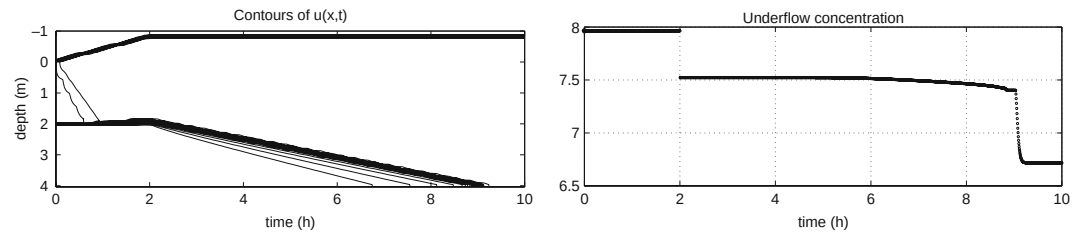

Figure 38. Optimal control with respect to CO3 as $(u_f, s) = (1{\cdot}8, 11{\cdot}0) \in \mathcal{D}(Q_{u0} = 3500) \cap \Lambda_{1a}$. The control action L1 with $Q_u = \tilde{Q}_u = 4631$ is performed at $t = 2$ h.

Sections 6.5 and 6.6) and $Q_u = Q_f$ for $(u_f, s) \in \Lambda'_b$ (see Section 6.8). In both cases optimal operation is left immediately. As is demonstrated in those sections, DCL1 (= DCL2 = DCL3) implies CO1 ($u_{cl} = 0$). Furthermore, CO2 and CO3 are equal. To satisfy these objectives, *i.e.*, maintaining $u_u = u_u^{min} = u_{u0}$ as long as possible, the first step-control action (L1 = L2 = L3) should be taken just before the SBL reaches the effluent level to keep $u_e = 0$.

8. Conclusions

The main purpose of a clarifier-thickener unit is that it should produce both a high underflow concentration and a zero effluent concentration. The main difficulty in the control of an ideal clarification-thickening process is that it is nonlinear with complex relations between concentrations and volume flows via the solution of a partial differential equation. The input variable is the feed point (u_f, s) consisting of the feed concentration and flux. The control variable is the volume flow Q_u of the underflow stream.

In order to approach the control problem, control objectives are defined in Section 4. In these, the concept of optimal operation is fundamental. This relates to a specific type of solution of the model partial differential equation, where there is a sludge blanket level (SBL), which is a discontinuity in the thickening zone separating low and high concentrations. Theorem 4.1 states that during optimal operation the underflow concentration can be kept above a given lower bound by keeping the control variable Q_u below a specific value, which depends on the bound. This value can be obtained graphically in the operating chart for control of steady states; see Figure 4. This also shows the interval of possible underflow concentrations during optimal operation. Based on the knowledge about the control of steady-state solutions in [1] and the step responses in [2], control strategies were introduced in Section 5. They state how the control variable Q_u should be set as a function of the feed point and time to meet each control objective.

In this paper we have focused on the control of the process for each possible step input and with respect to three control objectives. The first stage is to investigate the responses when a single step-control action is performed directly. The control variable is set to a value corresponding to a desired steady state (if possible optimal operation, otherwise a critically loaded settler). Such responses were classified in Section 6, where the operating chart in Figure 6 is divided into seven regions corresponding to the qualitatively different solutions. Unfortunately, it turns out that this single-step strategy is not always sufficient to satisfy the control objectives. For example, if the initial SBL is located near the bottom of the vessel and there is (even a small) step-input change such that the settler is going to be overloaded, then a direct control action may imply that optimal operation is left after a short time as the SBL reaches the bottom; see Figure 19.

The main results of the paper are the optimal control strategies presented in Section 7 by means of the operating chart in Figure 25 and the accompanying Table 2. This chart also contains seven regions, which, however, are different from the previous ones (Figure 6). An overall conclusion is that, for any step input, piecewise constant control with at most three step-control actions is sufficient to meet any of the control objectives.

All theoretically possible feed concentrations have been considered. In reality, only lower or intermediate feed concentrations are of interest. It is therefore interesting to note that, for feed concentrations in an arbitrary small interval around the characteristic concentration u_m, five of the seven regions of the optimal-control chart in Figure 25 are possible. This really illustrates the nonlinearity of the process and the difficulty in controlling it.

For all step responses with unchanged Q_u the underflow concentration and the solution in the bottom part of the thickening zone are unchanged until possibly the SBL reaches

the bottom (see [2]). All solutions in Section 6 can be regarded as step responses when also Q_u makes a jump. An interesting conclusion is then that the underflow concentration always makes a jump at $t = 0$ but the solution in the bottom part of the thickening zone changes only continuously until possibly the SBL reaches the bottom.

For intermediate feed concentrations and the two most common step inputs, the following can be concluded referring to the optimal-control chart in Figure 25. Firstly, if $(u_f, s) \in \mathcal{U}_1 \cap (P \cup \Lambda_2 \cup \Lambda_3)$, the settler is prevented from underloading by lowering the control variable Q_u. It turns out that this has a stabilizing effect on the SBL; the mass is unchanged and the underflow concentration makes a step increase directly and then stays constant. An explicit relation between the initial and the new SBL has been given; see (6) and Figure 9. Secondly, if $(u_f, s) \in \mathcal{O}_{2a} \cup (\mathcal{S} \cap \Lambda_3)$, the prevention of an overloaded settler is obtained by increasing Q_u. The sludge blanket declines initially and may reach the bottom if the initial depth is too low; see Figure 19. A safe margin is given by the inequality (9). Even for an initially higher SBL a step increase in Q_u may be disadvantageous since the underflow concentration decreases directly with a step and this may violate the given control objective. To satisfy the control objectives, one should delay any control action for a while; see Figures 28–30. In this case the initial SBL can actually be recovered with only one control action; see Figure 28.

A natural continuation of this series of papers is to generalize the results on step responses and control of these to a dynamic input and to present a regulator for the process.

The results presented in this series of papers have been obtained for ideal non-flocculated suspensions that obey Kynch's assumption. Many real slurries consist of flocculated suspensions that show a compressible behaviour at high concentrations and it would be interesting to see how the present results alter when compression is taken into account. The model equation will then have an additional diffusion term, which is non-zero only for concentrations above a critical concentration. Extensive analyses of such a strongly degenerate parabolic equation have been performed lately and, what concerns the modelling of continuous sedimentation in clarifier-thickener units, culminated in the recent paper [12] by Bürger *et al.*

Acknowledgement

I am grateful to Dr Anders Holst, Centre for Mathematical Sciences, Lund University, for reading and commenting upon parts of the manuscript.

References

1. S. Diehl, Operating charts for continuous sedimentation I: Control of steady states. *J. Engng. Math.* 41 (2001) 117–144.
2. S. Diehl, Operating charts for continuous sedimentation II: Step responses. *J. Engng. Math*. 53 (2005) 139–185.
3. H. Stehfest, An operational dynamic model of the final clarifier. *Trans. Inst. Meas. Control* 6(3) (1984) 160–164.
4. T.M. Keinath, Operational dynamics and control of secondary clarifiers. *J. Water Pollut. Control Fed.* 57 (1985) 770–776.
5. M.C. Bustos, F. Paiva and W. Wendland, Control of continuous sedimentation as an initial and boundary value problem. *Math. Methods Appl. Sci.* 12 (1990) 533–548.
6. N.G. Barton, C.-H. Li and J. Spencer, Control of a surface of discontinuity in continuous thickeners. *J. Austral. Math. Soc. Ser. B* 33 (1992) 269–289.
7. P. Balslev, C. Nickelsen and A. Lynggaard-Jensen, On-line flux-theory based control of secondary clarifiers. *Wat. Sci. Tech.* 30 (1994) 209–218.
8. J.-Ph. Chancelier, M. Cohen de Lara and F. Pacard, Analysis of a conservation PDE with discontinuous flux: A model of settler. *SIAM J. Appl. Math.* 54 (1994) 945–995.

9. J.-Ph. Chancelier, M. Cohen de Lara, C. Joannis and F. Pacard, New insight in dynamic modelling of a secondary settler – II. Dynamical analysis. *Wat. Res.* 31 (1997) 1857–1866.
10. S. Diehl, A conservation law with point source and discontinuous flux function modelling continuous sedimentation. *SIAM J. Appl. Math.* 56 (1996) 388–419.
11. S. Diehl and U. Jeppsson, A model of the settler coupled to the biological reactor. *Wat. Res.* 32 (1998) 331–342.
12. R. Bürger, K.H. Karlsen and J.D. Towers, A model of continuous sedimentation of flocculated suspensions in clarifier-thickener units. *SIAM. J. Appl. Math*. 65 (2005) 882–940.